antioxidants

Article

Glycine-Alanine Dipeptide Repeat Protein from C9-ALS Interacts with Sulfide Quinone Oxidoreductase (SQOR) to Induce the Activity of the NLRP3 Inflammasome in HMC3 Microglia: Irisflorentin Reverses This Interaction

Ru-Huei Fu [1,2,3,*,†], Hui-Jye Chen [1,†] and Syuan-Yu Hong [1,4,5]

[1] Graduate Institute of Biomedical Sciences, China Medical University, Taichung 40402, Taiwan
[2] Translational Medicine Research Center, China Medical University Hospital, Taichung 40447, Taiwan
[3] Ph.D. Program for Aging, China Medical University, Taichung 40402, Taiwan
[4] Department of Medicine, School of Medicine, China Medical University, Taichung 40447, Taiwan
[5] Division of Pediatric Neurology, China Medical University Children's Hospital, Taichung 40447, Taiwan
* Correspondence: rhfu@mail.cmu.edu.tw; Tel.: +886-422052121-7826
† These authors contributed equally to this work.

Abstract: Amyotrophic lateral sclerosis (ALS) is a fatal rare disease of progressive degeneration of motor neurons. The most common genetic mutation in ALS is the hexanucleotide repeat expansion (HRE) located in the first intron of the C9orf72 gene (C9-ALS). HRE can produce dipeptide repeat proteins (DPRs) such as poly glycine-alanine (GA) in a repeat-associated non-ATG (RAN) translation. GA-DPR has been shown to be toxic to motor neurons in various biological models. However, its effects on microglia involved in C9-ALS have not been reported. Here, we show that GA-DPR (GA_{50}) activates the NLR family pyrin domain containing 3 (NLRP3) inflammasome in a human HMC3 microglia model. MCC950 (specific inhibitor of the NLRP3) treatment can abrogate this activity. Next, using yeast two-hybrid screening, we identified sulfide quinone oxidoreductase (SQOR) as a GA_{50} interacting protein. SQOR knockdown in HMC3 cells can significantly induce the activity of the NLRP3 inflammasome by upregulating the level of intracellular reactive oxygen species and the cytoplasmic escape of mitochondrial DNA. Furthermore, we obtained irisflorentin as an effective blocker of the interaction between SQOR and GA_{50}, thus inhibiting NLRP3 inflammasome activity in GA_{50}-expressing HMC3 cells. These results imply the association of GA-DPR, SQOR, and NLRP3 inflammasomes in microglia and establish a treatment strategy for C9-ALS with irisflorentin.

Keywords: amyotrophic lateral sclerosis (ALS); C9ORF72; glycine-alanine dipeptide repeat proteins (GA-DPRs); NLRP3 inflammasome; sulfide quinone oxidoreductase (SQOR); ROS; mitochondria DNA; irisflorentin

Citation: Fu, R.-H.; Chen, H.-J.; Hong, S.-Y. Glycine-Alanine Dipeptide Repeat Protein from C9-ALS Interacts with Sulfide Quinone Oxidoreductase (SQOR) to Induce the Activity of the NLRP3 Inflammasome in HMC3 Microglia: Irisflorentin Reverses This Interaction. *Antioxidants* **2023**, *12*, 1896. https://doi.org/10.3390/antiox12101896

Academic Editors: Reto Asmis, Marco Bisaglia and Sasanka Chakrabarti

Received: 31 August 2023
Revised: 7 October 2023
Accepted: 18 October 2023
Published: 23 October 2023

1. Introduction

Amyotrophic lateral sclerosis (ALS), a motor neuron disease (MND), causes progressive degeneration of the upper and lower motor neurons in the brain and spinal cord. Muscle stiffness, twitching, and atrophy are the characteristics of this disease. Progressive deterioration of speaking and swallowing ability eventually leads to respiratory failure. The average survival period of ALS from onset to death is approximately 3–5 years. The disease affects about 7.7 out of every 100,000 Americans each year and is most common among white men aged 60–69 [1]. At present, there is no effective method to delay the establishment of the disease and cure ALS. Although the drug riluzole has been approved, it only extends life by about two to three months and does not reverse the activity of damaged motor neurons [2].

ALS has an unknown cause in 90–95% of cases (sporadic ALS). Approximately 5–10% of cases are genetically related (familial ALS). To date, many genetic mutations associated

with ALS have been identified, including *C9orf72*, *SOD1*, *FUS*, *TARDBP/TDP-43*, *ANG*, *SETX*, *ALS2*, and *VAPB*. These genetic variants also contribute to the development of sporadic ALS [3,4]. *C9orf72* is the most common genetic variant (40%, familial ALS) and occurs in a high proportion (8–10%) of sporadic ALS patients [5]. This gene is highly expressed in ALS-associated motor neuron populations [6,7]. In a normal person, intron one of *C9orf72* contains, at most, 20–30 hexanucleotide repeats (GGGGCC; G_4C_2), but, in people with *C9orf72*-associated ALS (C9-ALS), this number can expand to hundreds to several thousand repeats, which is called hexanucleotide repeat expansion (HRE) [8,9].

The mechanisms by which HREs cause disease are still poorly understood. The loss of function (haploinsufficiency) and gain of function (either toxic RNA or protein products) in C9-ALS molecular pathology have been confirmed by related studies [10,11]. C9ORF72 protein is mainly distributed in the cytoplasm or synapses of cerebral cortex neurons and brain/spinal cord motor neurons [12]. Its loss may be related to the defect of endosomal trafficking, autophagy [13], axonal synapse, suppression of inflammation and autoimmunity [14], translation, unfolded protein response, and stress granule (SG) formation [15]. In the gain of function, aberrant RNAs containing extended HREs can block many functions in the nucleus [16] or be translated by an unconventional method called the repeat-associated non-ATG mechanism (RAN) [17–20]. This resulted in five dipeptide repeat proteins (DPR) (Gly-Ala, Gly-Pro, Gly-Arg, Pro-Ala, and Pro-Arg) from ribosomal reading frames of sense or antisense directions generated and accumulated in the central nervous system of patients with C9-ALS [21]. However, studies have shown that only poly-GA has the highest expression in the brains of patients with C9-ALS [22], and its distribution is very similar to the neuronal cytoplasmic insoluble and ubiquitinated p62-positive inclusions usually observed in patients [23].

GA-DPR is cytotoxic and causes dysfunction of the ubiquitin–proteasome system [24], caspase-3 activation (apoptosis), damage of neurite outgrowth, endoplasmic reticulum stress [25], nuclear membrane destruction, obstruction of nucleocytoplasmic transport [26], and TDP-43 cleavage [27]/aggregation [28] in neuronal cells. GA-DPR also depletes the level of soluble Unc119, inhibits dendritic arborization, and leads to apoptosis of primary neurons [29]. Other studies have shown that if GA aggregates exist in neurites in mouse models and patient-induced pluripotent stem cell lines, they will reduce synaptic vesicle-associated protein 2 (SV2) levels and affect Ca^{2+}influx and synaptic vesicle release, ultimately affecting synaptic function [22]. In *C. elegans* models, GA-DPR induces neurodegeneration, leading to movement impairments. Simultaneously exhibits longevity defects [30].

Current research shows that C9-ALS may abnormally activate the immune system [31]. Gut bacteria-induced systemic and neuroinflammation mediated by TMEM173-induced type I interferon has been observed in C9-ALS mice [32]. Synthesis of pro-inflammatory chemokines and cytokines was also found to be upregulated in the CSF and serum of C9-ALS patients [33]. Recent evidence revealed that, in addition to motor neurons, microglia may also be the primary cell responsible for ALS [34]. Furthermore, interferon-responsive proinflammatory microglial activation was characterized by transcriptome analysis in GA-DPR mice and C9-ALS patients [35]. Notably, NLRP3 (NOD-, LRR-, and pyrin domain 3) inflammasome activation in microglia is frequently observed in ALS-associated neuroinflammation in patient and mouse models [36]. It induces the activation of caspase 1 and then promotes the maturation and release of the pro-inflammatory cytokines IL-1β and IL-18, as well as activating gasdermin D-dependent pyroptosis [37]. Here, we were interested in whether *C9orf72*-associated GA-DPR stimulated microglial NLRP3 inflammasome activity, leading to ALS symptoms. Our results showed that endogenous GA_{50} can effectively cause NLRP3 inflammasome activation in HMC3 cells (human microglial cell line). In addition, we also confirmed that the activity induction was partly caused by the interaction affecting the function of sulfide quinone oxidoreductase (SQOR, GenBank: NM_001271213) protein, resulting in mitochondrial ROS generation and cytoplasmic escape of mitochondrial DNA. Finally, we found that the favonoid "irisflorentin" from *Belamcanda*

chinensis (L.) DC could block the interaction between GA-DPR and SQOR and showed the potential to ameliorate C9-ALS-associated GA-DPR toxicity in cell models. Irisflorentin has the opportunity to be a potential option for the treatment of C9-ALS.

2. Materials and Methods

2.1. Chemicals and Maintenance of HMC3 Cell Lines

Chemicals used in this study were purchased from Sigma-Aldrich (St. Louis, MO, USA) unless otherwise stated. Reagents and media were acquired from Gibco (Thermo Fisher Scientific, Waltham, MA, USA). HMC3 human microglia were provided by Shao-Chih Chiu (China Medical University, Taichung, Taiwan). Cell cultures were performed as described in previous publications [38].

2.2. Construction and Transfection of Plasmid

Coding DNA for GA_{50} and SQOR was synthesized by Genewiz (South Plainfield, NJ, USA). The DNA of GA_{50} was cloned into the pcDNA 3.1/myc-His vector (Invitrogen, Waltham, MA, USA), pGBKT7 vector (Clontech, Mountain View, CA, USA), pGADT7 vector (Clontech), pCMV -Myc (Clontech), or pCMV-HA (Clontech). The SQOR fragment was inserted into pGBKT7, pGADT7, pCMV-Myc, or pCMV-HA vectors. Plasmids were transfected into HMC3 or 293T cell lines using Lipofectamine 2000 reagent (Invitrogen) according to the manufacturer's protocols. Transfectants were selected using G418 (1.5 mg/mL). Yeast transformation for the pGBKT7 or pGADT7 plasmid was performed using Quick and Easy Transformation Mix (Clontech) according to the manufacturer's protocol.

2.3. Immunofluorescence Analysis of HMC3 Cells

Immunofluorescence staining was performed according to our previously published protocol [38]. In short, cells adhered to the coverslip were fixed using paraformaldehyde (4%), followed by permeation with Triton X-100 (0.2%). The coverslips were then blocked in a milk solution, and then primary antibody was added to swing overnight (4 °C). The next day, the washed cells were added to Alexa Fluor 488-linked anti-mouse and Alexa Fluor 568-linked anti-rabbit secondary antibodies (both from goat, Invitrogen) at 25 °C for 1 h. Afterwards, cells were washed, and DAPI was used to stain nuclei. Finally, the fluorescence signal was observed using a fluorescence microscope. Myc, SQOR, and NF-κB p65 antibodies were obtained from Cell Signaling Technology (Beverly, MA, USA).

2.4. Acquirements of Nuclear Extracts and Transcription Factor Assay of NF-κB p65 in HMC3 Cells

We used the nuclear extraction kit (Sigma-Aldrich) to extract proteins in the nucleus according to the manufacturer's manual. For the activity assay of NFκBp65, we employed the NFκB p65 EZ-TFA Transcription Factor Assay Colorimetric Kit purchased form Millipore (Temecula, CA, USA) according to the instruction manual.

2.5. Protein Extraction and Western Blot Analysis of HMC3 Cells

Protein extraction and Western blotting were performed using the experimental method described in the previous literature [38]. In summary, we added RIPA buffer (Millipore) containing aprotinin, leupeptin, PMSF, and phosphatase inhibitors to culture cells. The cells were then scraped, and cell lysates were collected. For Western blotting, we loaded cell lysates (50 μg) onto 7.5–12.5% SDS-PAGE for analysis. The location and signal intensity of specific proteins in PVDF membranes were determined using an ECL reagent (Amersham Biosciences, Piscataway, NJ, USA) and a luminescence imaging sensor (UVP, Upland, CA, USA). Primary antibodies, including NF-κB p65, NLPR3, ASC, caspase 1, IL-1β, IL-18, and GAPDH, were obtained from Cell Signaling Technology. HRP-linked anti-rabbit and anti-mouse secondary antibodies (both from goat) were acquired from PerkinElmer, Inc. (Boston, MA, USA).

2.6. Analysis of IL-1β and IL-18 in the Conditioned Media of HMC3 Cells

Conditioned medium from HMC3 cells was centrifuged at low speed (1000× *g*, 5 min), and the supernatant was collected and passed through a filter tip (0.22 μm) to remove cell debris. Next, IL-1β, IL-18, and c-Myc ELISA were performed according to the manufacturer's instructions (invitrogen). Each sample was tested with 50 μL of conditioned medium and quantified on a microplate reader.

2.7. In Situ TUNEL Analysis of HMC3 Cells

The number of HMC3 cells exhibiting apoptosis in situ was counted using the Click-iT™ Plus TUNEL Assay Kit (invitrogen) according to the manufacturer's instructions. Briefly, after fixation (4% paraformaldehyde) and permeabilization (0.25% Triton™ X-100/PBS), cells on coverslips were incubated with Tdt reaction mixture for 60 min. Next, Click-iT™ plus TUNEL reaction mix (containing Alexa Fluor™ 488 dye) was added to cells for 30 min in the dark. Finally, the number of apoptotic cells was observed and counted with a fluorescent microscope.

2.8. Detection of Apoptosis in HMC3 Cells by Flow Cytometry

Apoptosis analysis was performed using the FITC Annexin-V Apoptosis Detection Kit I (BD Biosciences Pharmingen, San Diego, CA, USA) according to the manufacturer's protocol. Briefly, we added 100 μL of binding buffer to cells harvested after washing. Next, cells were stained with annexin-V FITC and PI for 15 min in the dark. Then, 400 μL of binding buffer was added, and the ratio of apoptotic cells was immediately determined using a flow cytometer. The gate for cell collection was set to contain 10,000 events per sample.

2.9. HMC3 Cells Were Treated with Inhibitor of NLRP3 Inflammasome

MCC950, a dairylsulfonylurea compound, is a potent and selective inhibitor of the NLRP3 inflammasome. We incubated GA_{50}-transfected HMC3 cells in fresh medium containing MCC950 for 24 h prior to analysis.

2.10. Using a Yeast Two-Hybrid Library to Screen GA-DPR-Interacting Proteins

The Matchmaker cDNA library construction of HMC3 cells and the two-hybrid assay of Matchmaker GAL4 were performed according to the operation manual provided by the manufacturer (Clontech). Briefly, we transformed the pGBKT7/GA_{50} plasmid into the AH109 strain of *Saccharomyces cerevisiae* and the HMC3 cell cDNA library constructed in the pGADT7 vector into the Y187 strain. Next, the bait train and library strains were mated to generate diploids. Finally, the interaction of GA_{50} with candidate proteins can be confirmed by the positive clones on SD/-Ade/-His/-Leu/-Trp X-α-gal plates. In addition, we recovered the pGADT7 plasmid from positive yeast clones using a yeast plasmid miniprep I kit from Zymo Research Corporation (Irvine, CA, USA) and sequenced it to identify the interaction genes.

2.11. Yeast Two-Hybrid Assay of GA_{50} and SQOR

We subcloned GA_{50} and SQOR DNA fragments into pGBKT7 or pGADT7 vectors. Next, pGBKT7 or pGADT7 plasmids were transformed into AH109 and Y187 yeast strains. Finally, we performed a two-hybrid assay of Matchmaker GAL4, the procedure of which is described in Section 2.10.

2.12. Co-Immunoprecipitation Analysis of GA_{50} and SQOR

We refer to the experimental procedures described in the previously published literature for co-immunoprecipitation analysis [38]. First, the pCMV/GA_{50}/Myc plasmid and pCMV/SQOR/HA plasmid were co-transfected into 293 T cells according to the transfection method described in Section 2.2. After 24 h, cell lysates were collected using Pierce™ IP Lysis Buffer (Thermo Fisher Scientific). Next, supernatants were immunoprecipitated with anti-Myc-Tag antibody or normal immunoglobulin G from rabbits for 2 h (4 °C).

Beads of Protein G-Sepharose were then added for 1 h. Finally, the co-immunoprecipitation complexes were washed and identified by Western blotting using mouse anti-HA-Tag monoclonal antibody (Cell Signaling Technology). In addition, we performed immunoprecipitation of cell lysates with mouse anti-HA-tag monoclonal antibody and Western blotting with rabbit anti-Myc-tag monoclonal antibody. In another set of experiments, we co-transfected pCMV/SQOR/Myc plasmids and pCMV/GA50/HA plasmids into 293T cells and performed co-immunoprecipitation as described above.

2.13. siRNA Treatment of SQOR in HMC3 Cells

HMC3 cells were seeded on culture plates (6-well, 2.0×10^5 cells/well) and grown to 70% confluence. SQOR siRNA (75 nM) or non-targeting control siRNA were then delivered into cells using Lipofectamine 2000 Reagent (Invitrogen) according to the producer's protocol. After 24 h, cells and media were harvested for subsequent experiments. SQOR siRNA was purchased from Sigma-Aldrich and its product number is EHU032561.

2.14. Reactive Oxygen Species (ROS) Assay in HMC3 Cells

We measured intracellular ROS levels using a permeable H2DCFDA (DCFH-DA) (Sigma-Aldrich) probe as a marker according to a method previously described [39]. The fluorescence intensity of the probe after cell staining can be observed by fluorescence microscopy and detected by flow cytometry.

2.15. Measurement and Quantification of Cytoplasmic mtDNA in HMC3 Cells

We measured cytoplasmic mtDNA by general PCR or RT-qPCR analysis according to the experimental procedures described in the published literature [39]. In brief, half of the cells in each group were lysed with mild lysis buffer (containing 0.1% NP-40) and the other half with strong lysis buffer (containing 0.1% NP-40 and 0.1% SDS). Cells were treated with lysis buffer on ice and centrifuged at 4 °C. Next, the supernatant was passed through a Genomic DNA isolation kit (Sigma-Aldrich) to purify cytoplasmic mtDNA and total cellular DNA. Finally, we used PCR and RT-qPCR for analysis. The ratio of mtDNA to total DNA reflects the degree of cytoplasmic DNA escape.

2.16. Irisflorentin Treatment and Growth Assay of a Yeast Two-Hybrid Based on the Interaction between GA_{50} and SQOR

Synthetic irisflorentin (IFT, mol. wt. 386.35, 98% purity) was prepared as a 100 mM stock solution (in DMSO) and stored at −20 °C. Diploid yeast carrying BD-/AD-, BD-p53/AD-T, BD-GA_{50}/AD-S3 (SQOR), or BD-S3/AD-GA_{50}, respectively, were cultured in SD/-Leu/-Trp broth containing serially diluted IFT overnight until they reached the log or mid-log phase (30 °C). In the yeast spot assay, we normalized the diploid cultures. Next, serial dilutions were made and spotted (10 µL) onto non-selective (SD/-Leu/-Trp) or selective (SD/-Ade/-His/-Leu/-Trp) dishes and grown at 30 °C for 3 days. In absorbance assay experiments, diploid cultures from each group were normalized and cultured in non-selective or selective broth with serial dilution IFT. OD values were recorded every 12 h during the 48 h experiment.

2.17. Toxicity Analysis and Treatment of Irisflorentin on HMC3 Cells

The toxicity of irisflorentin to HMC3 cells was confirmed using an MTT cell survival assay. We treated HMC3 cells for 24 h with serial dilutions of IFT. The cells were then replaced with fresh medium and incubated with MTT (5 mg/mL) at 37 °C for 2 h. Finally, the cells were washed with isopropanol. Cell viability was quantified using a spectrophotometer. On IFT treatment, we replaced GA50-expressing HMC3 cells with fresh medium and treated them with IFT for 24 h, then collected cells and conditioned medium for subsequent experiments.

2.18. Statistical Work on the Data for This Study

Each work in this study was implemented in triplicate. We used SAS software 9.3 (SAS, Institute. Inc., Cary, NC, USA) for general statistical analysis of the data of this study. Study data are presented as mean ± standard deviation (SD). Furthermore, statistical significance was determined by using one-way analysis of variance (ANOVA) and Tukey's test. Again, comparisons between two groups were performed using Student's *t*-test. Statistical significance is indicated with a p-value < 0.05.

3. Results

3.1. Expression of Glycine-Alanine-Dipeptide Repeat Protein (GA-DPR) Causes NLRP3 Inflammasome Activity in a Human HMC3 Microglia Cell Model

The mechanism of the NLRP3 inflammasome involves the activation of NF-κB and the formation of mature caspase-1, mature IL-1β, and mature IL-18 (mIL-18) [32]. First, we investigated whether glycine-alanine dipeptide repeat protein (GA-DPR) could cause NLRP3 inflammasome activity in microglia. We expressed GA-DPR (GA_{50}) by transient transfection in a human HMC3 microglial cell line. After 24 h of transfection by immunofluorescence analysis, we found that GA50 was mainly distributed in the cytoplasm to form aggregates (Figure 1A). In addition, Western blot analysis showed that the expression of GA_{50} increased the amount of NF-κB p65 in the nucleus ($p < 0.001$, Figure 1B). Likewise, ELISA analysis of transcription factors showed ($p < 0.001$, Figure 1C) that expression of GA_{50} could significantly induce NF-κB p65 activity. These findings indicated priming of the NLRP3 inflammasome.

Furthermore, our Western blot analysis showed that the expression of GA50 could significantly increase the expression of NLRP3 ($p < 0.001$), ASC ($p < 0.001$), mature caspase 1 (p20) ($p < 0.001$), pro-IL-1β ($p < 0.001$), mature IL-1β (p17) ($p < 0.001$), pro-IL-18 ($p < 0.001$), and mature IL-18 ($p < 0.001$) levels (Figure 1D). ELISA assays revealed increased secretion of mature IL-1β ($p < 0.0001$) and mature IL-18 ($p = 0.0002$) in the conditional medium (GA-CM) of GA_{50}-expressing HMC3 cells (Figure 1E). The above data indicate that intracellularly expressed GA_{50} can induce the activation of NLRP3 inflammasome in HMC3 microglia.

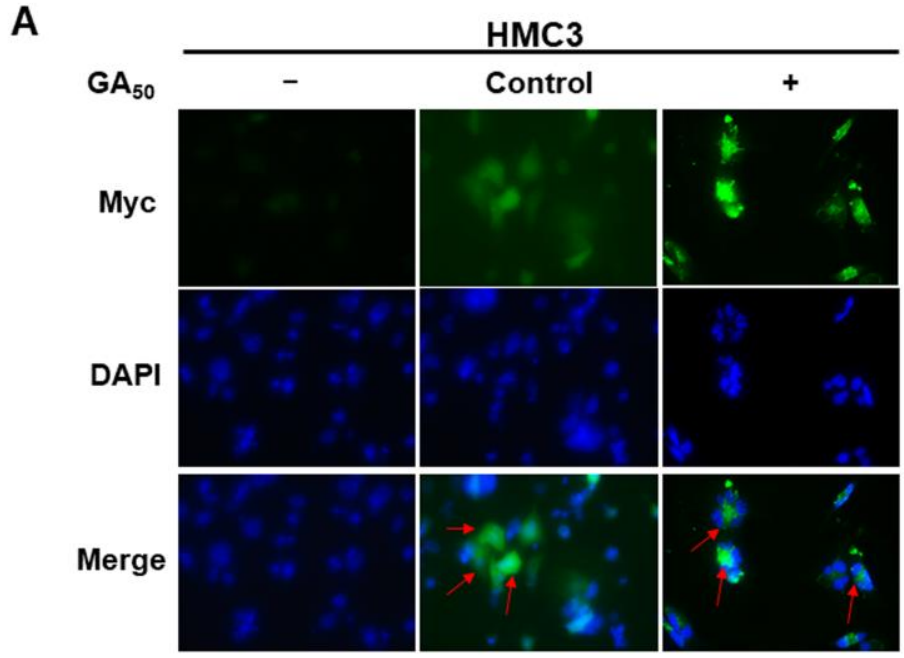

Figure 1. *Cont.*

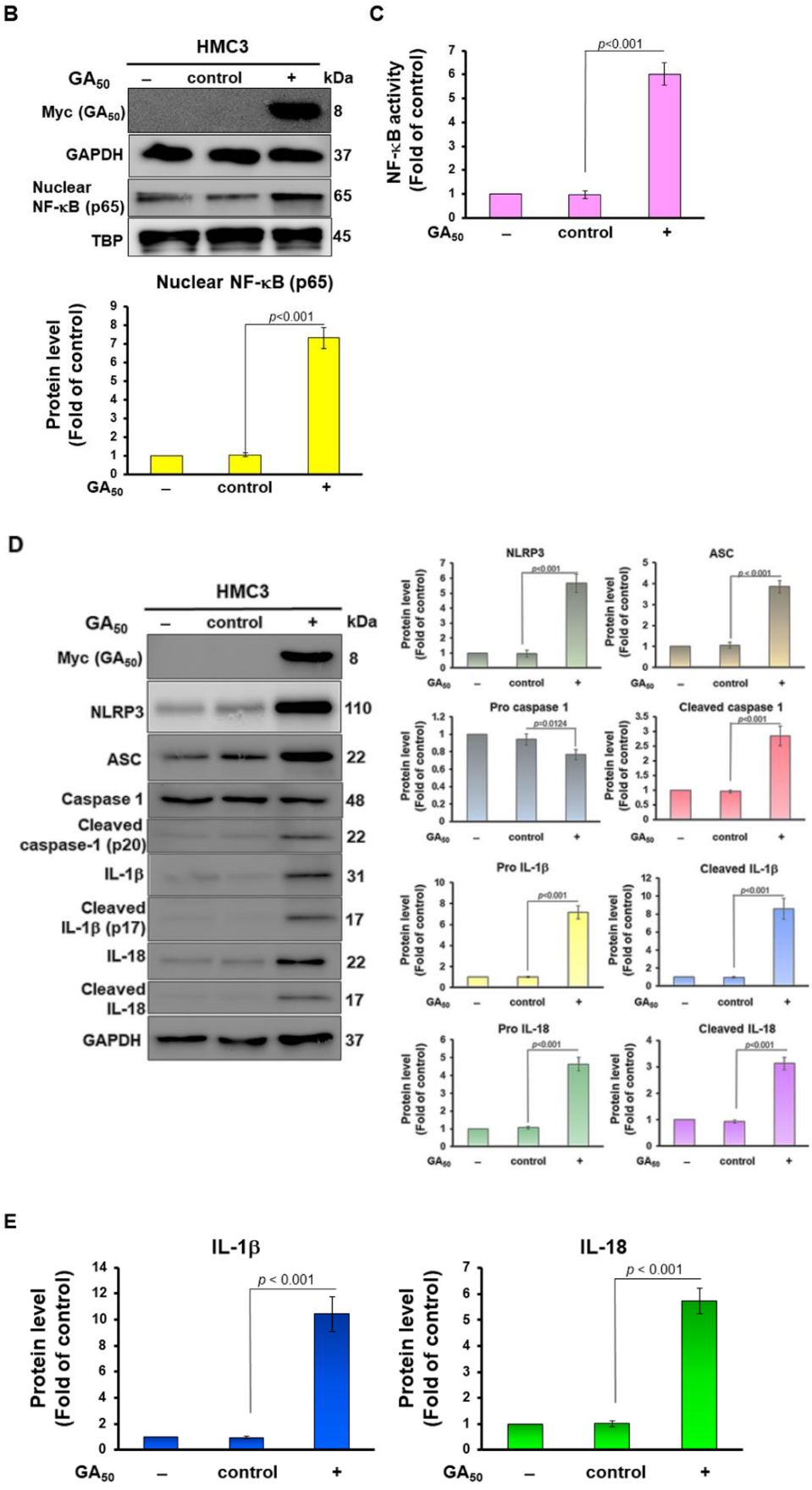

Figure 1. *Cont.*

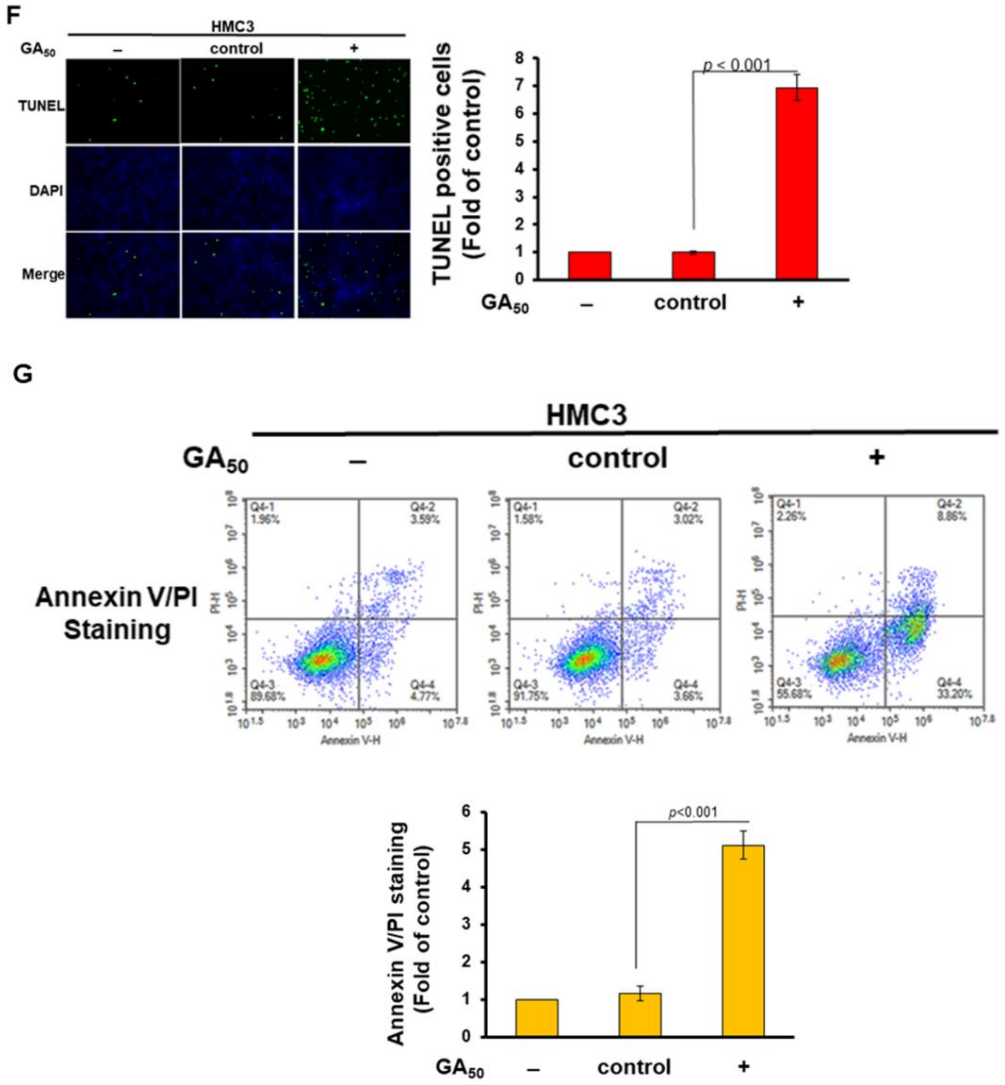

Figure 1. Intracellular expression of GA50 in human HMC3 microglia leads to NLRP3 inflammasome activation. The control vector or GA_{50} plasmid was transfected into HMC3 cells for 24 h. (**A**) Immunofluorescence staining of GA_{50} using anti-Myc-tag antibody (green). The location of the nuclei was confirmed by DAPI staining. The magnification of a microscope is 400X. GA_{50} mainly forms aggregates in the cytoplasm (red arrows). (**B**) The amount of NF-κB p65 in the nucleus was evaluated by Western blotting and quantified using ImageJ software (version 1.53). TBP protein is an internal loading control. (**C**) ELISA analysis quantifies the transcriptional activity of NF-κB p65. (**D**) Expression of GA_{50} (Myc), NLRP3, ASC, caspase-1, IL-1β, and IL-18 in cell lysates was analyzed by Western blot and quantified using ImageJ software (version 1.53). GAPDH was employed as an internal loading control. (**E**) The amount of IL-1β and IL-18 secreted in conditional media was determined using ELISA assay. (**F**) The number of cells with chromosomal breaks was estimated using TUNEL assay. The magnification of a microscope is 100X. (**G**) Ratios of pyroptosis cell were determined by flow cytometry with annexin v-FITC and propidium iodide (PI) staining. The histogram shows the pyroptosis rate [(Q1 + Q2)/(Q1 + Q2 + Q3 + Q4) × 100%].

As activation of the NLRP3 inflammasome causes cellular pyroptosis [36], we wanted to assess whether expression of GA_{50} in HMC3 cells would increase cellular pyroptosis. The TUNEL assay showed that the number of positive cells was significantly increased under GA_{50} expression ($p < 0.001$, Figure 1F). We then quantified annexin V/propidium iodide (PI) staining by flow cytometry and found that GA_{50} expression increased the ratio of pyroptosis cells ($p < 0.001$, Figure 1G).

3.2. Exocytosis of Mature IL-1 β and IL-18 in GA_{50}-Expressing HMC3 Cells Was Inhibited by Treatment with MCC950 Inhibitor of the NLRP3 Inflammasome

To further identity that expression of GA_{50} activates the NLRP3 inflammasome of HMC3 cells, we used an MCC950 inhibitor of the NLPR3 inflammasome. The results showed that after 100 nM MCC950 treatment, the levels of NLRP3 and ASC did not change compared with the untreated group (Figure 2A). Nevertheless, the levels of cleaved caspase 1 ($p20$) ($p < 0.001$), cleaved IL-1β (p17)/pro IL-1β ($p < 0.001$), and cleaved IL-18/pro IL-18 ($p < 0.001$) meaningfully lowered (Figure 2A). Furthermore, we found that exocrine mature IL-1β ($p < 0.001$) and mature IL-18 ($p < 0.001$) were also significantly reduced (Figure 2B). These data confirm that the activity of the NLRP3 inflammasome in HMC3 microglia can be induced by GA-DPR.

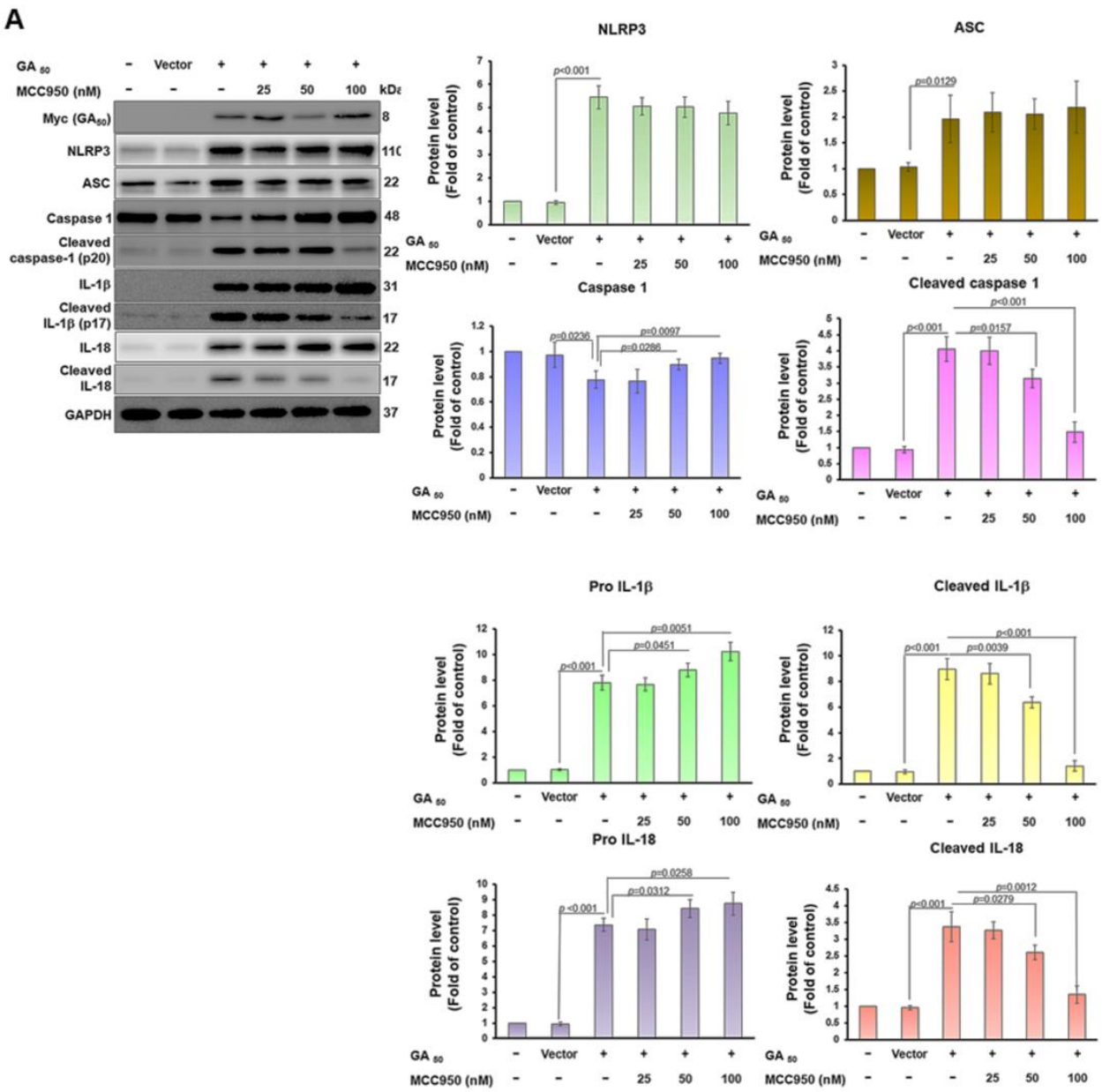

Figure 2. *Cont.*

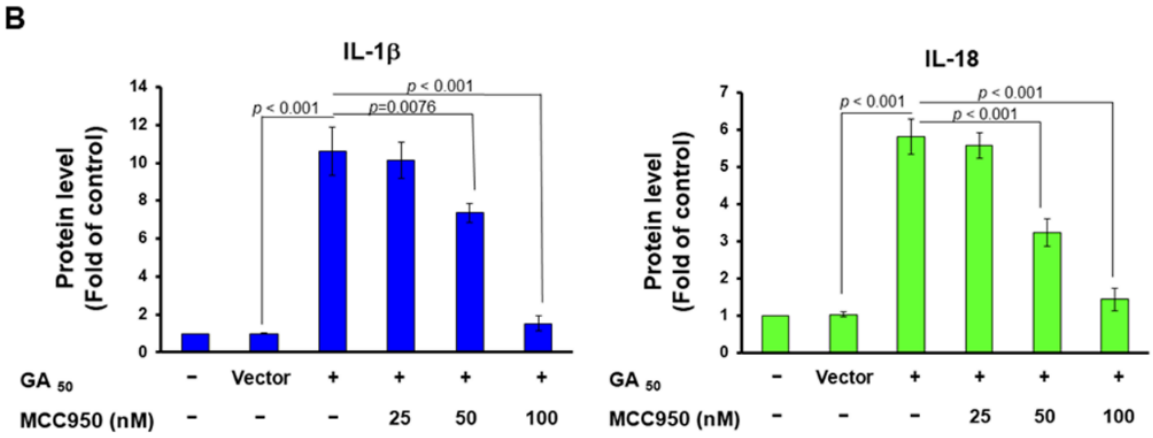

Figure 2. The activity of the NLRP3 inflammasome in GA_{50}-expressing HMC3 microglia can be inhibited by MCC950. HMC3 cells that expressed GA_{50} were treated with 0, 25, 50, or 100 nM MCC950 for 24 h. (**A**) Protein levels of GA_{50} (Myc) and NLRP3 inflammasome-associated components in cell lysates detected by Western blot analysis. The internal loading control was GAPDH protein. (**B**) The conditional medium was used to measure the secretion of mature IL-1β and mature IL-18 by ELISA.

3.3. GA-DPR Interacts with Sulfide Quinone Oxidoreductase (SQOR) in HMC3 Microglia

To explore the potential pathways by which GA-DPR activates the NLRP3 inflammasome in microglia, we sought the proteins that might associate with GA_{50} in HMC3 cells. First, we developed a cDNA expression library of HMC3 cells and performed yeast two-hybrid screening using GA_{50} as bait (Figure 3A). Among the positive clones that interacted with GA50, it was confirmed by sequencing that three blue clones included partial cDNA of sulfide quinone oxidoreductase gene (*SQOR*) (NCBI reference sequence: NP_067022.1) (Figure 3B,C).

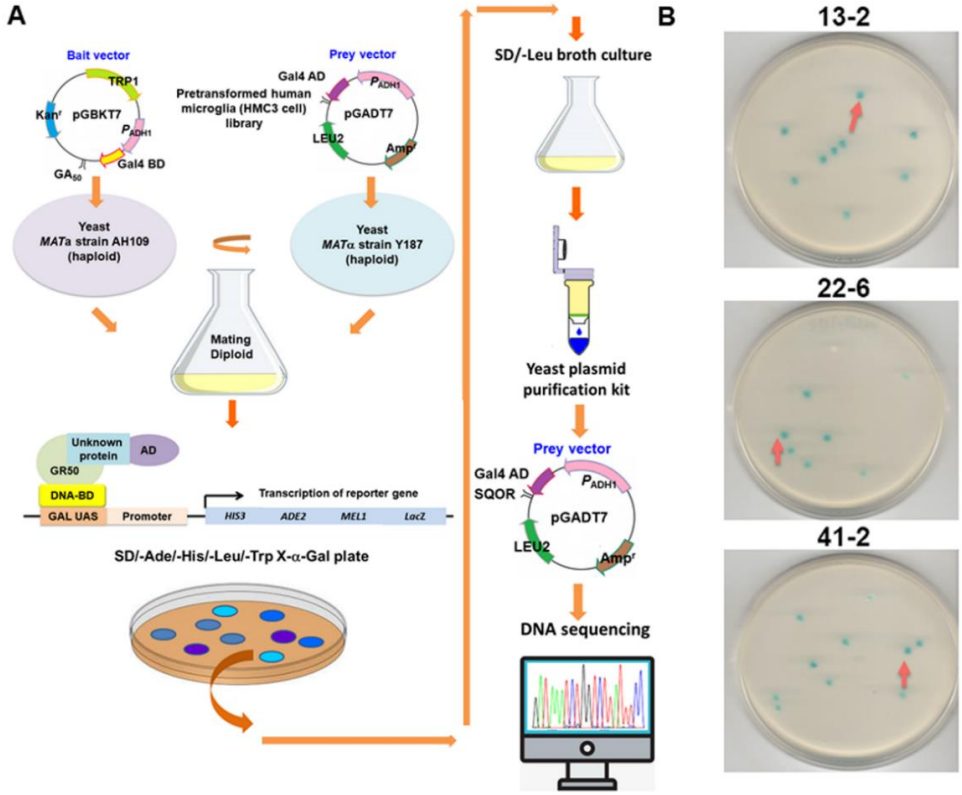

Figure 3. *Cont.*

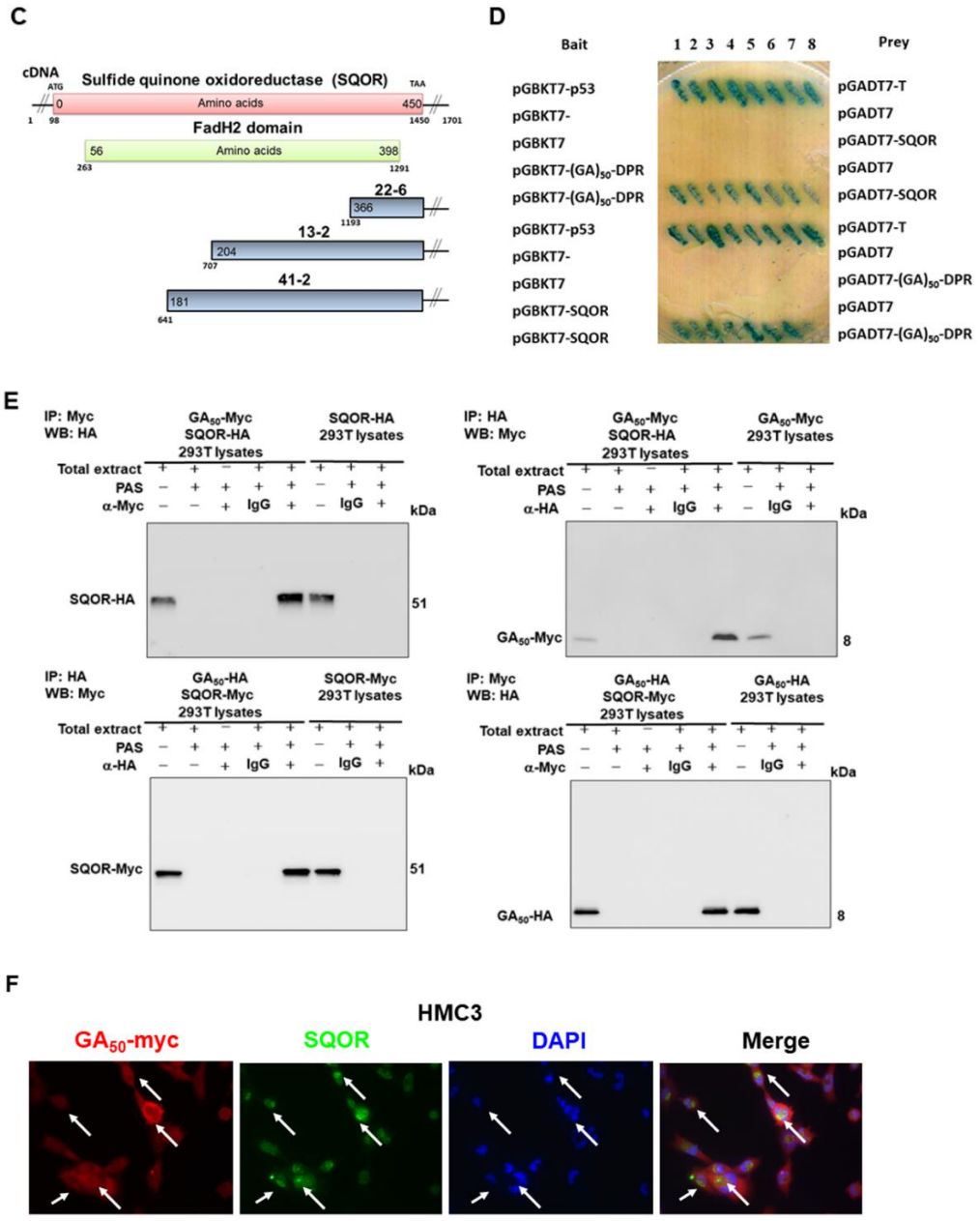

Figure 3. GA-DPR specifically interacts with sulfide quinone oxidoreductase (SQOR) in HMC3 cells. (**A**) Flowchart showing the yeast two-hybrid screening strategy, using GA_{50} as a bait to search for potential interacting proteins in a human HMC3 microglia cDNA library. (**B**) The reporter gene activated by the interaction induces the growth of blue diploid yeast containing positive clones of the *SQOR* cDNA fragment (red arrows). (**C**) Schematic representation of three cDNA clones spanning the coding sequence of the *SQOR* gene (NCBI reference sequence: NP_067022.1). SQOR comprises the FadH2 domain: sulfur reductase. (**D**) The interaction of GA_{50} with full-length SQOR was confirmed using the yeast two-hybrid assay. The positive control group was diploid yeast expressing BD-p53 and AD-T. (**E**) Confirmation of GA_{50} interaction with SQOR using co-immunoprecipitation analysis. 293T cells transfected with only one plasmid were used as a negative control. (**F**) Analysis using immunofluorescence staining confirmed that GA_{50} and SQOR are partially colocalized in the cytoplasm of HMC3 cells (white arrows). DAPI was used to stain the nuclei.

Next, we implemented a yeast two-hybrid assay of GA_{50} with full-length SQOR and observed the formation of prominent blue colonies (Figure 3D). We then co-expressed GA_{50} and SQOR fused to HA or Myc tags in 293T cells and performed co-immunoprecipitation.

The results showed that GA_{50} and SQOR could be identified in the co-immunoprecipitated complex (Figure 3E). Furthermore, we observed that GA_{50} partially co-localized with SQOR in the cytoplasm using immunofluorescence staining (Figure 3F). On the basis of these results, we determined that SQOR could interact with GA_{50}. To further confirm the precise interaction region, amino acid sequence of SQOR was divided into three independent fragments, including 1–150 (S1), 151–300 (S2), and 301–450 (S3), and implemented a yeast two-hybrid test with $GA_{50,}$ respectively (Figure 4A). The data showed that GA_{50} primarily associated with the S3 fragment of SQOR (Figure 4B–D).

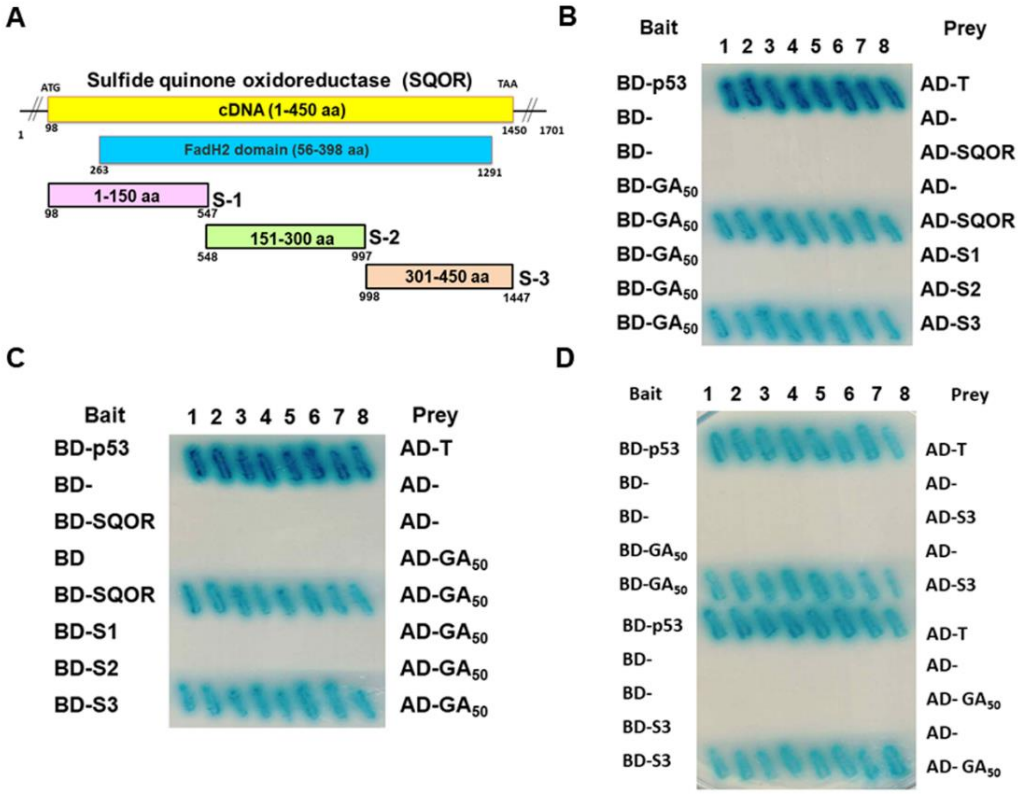

Figure 4. Confirmation of the C-terminus of SQOR as the major interaction region of GA_{50} by the yeast two-hybrid test. (**A**) Schematic showing that SQOR is divided into three fragments for the yeast two-hybrid test. (**B**–**D**) GA_{50} only interacts with the S3 fragment of SQOR in the yeast two-hybrid assay. The positive control was diploid yeast expressing BD-p53 and AD-T.

3.4. Downregulation of SQOR Expression in HMC3 Microglia Activates NLRP3 Inflammasome

As SQOR interacts with GA_{50}, it is unclear whether this effect mediates NLRP3 inflammasome activity. Therefore, we clarified the role of SQOR expression on NLRP3 inflammasome activation in HMC3 cells. We downregulated the level of SQOR in HMC3 cells using siRNA. Western blot analysis showed that the level of SQOR was significantly decreased in HMC3 cells after *SQOR* siRNA treatment compared with the control siRNA group ($p < 0.001$, Figure 5A). In contrast, in the *SQOR* siRNA group, NLRP3 ($p < 0.001$), ASC ($p = 0.007$), cleaved caspase 1 ($p < 0.001$), pro IL-1β ($p < 0.001$), cleaved IL-1β ($p < 0.001$), pro IL-18 ($p < 0.001$), and cleaved IL-18 ($p < 0.001$) were all significantly increased compared to the control siRNA group (Figure 5A). On the ELISA analysis of conditioned media, the exocytosis of mature IL-1β ($p < 0.001$) and mature IL-18 ($p < 0.001$) was significantly increased in the *SQOR* siRNA group compared with the control siRNA group (Figure 5B). Those results revealed that the inhibition of SQOR expression can activate NLRP3 inflammasome in HMC3 cells.

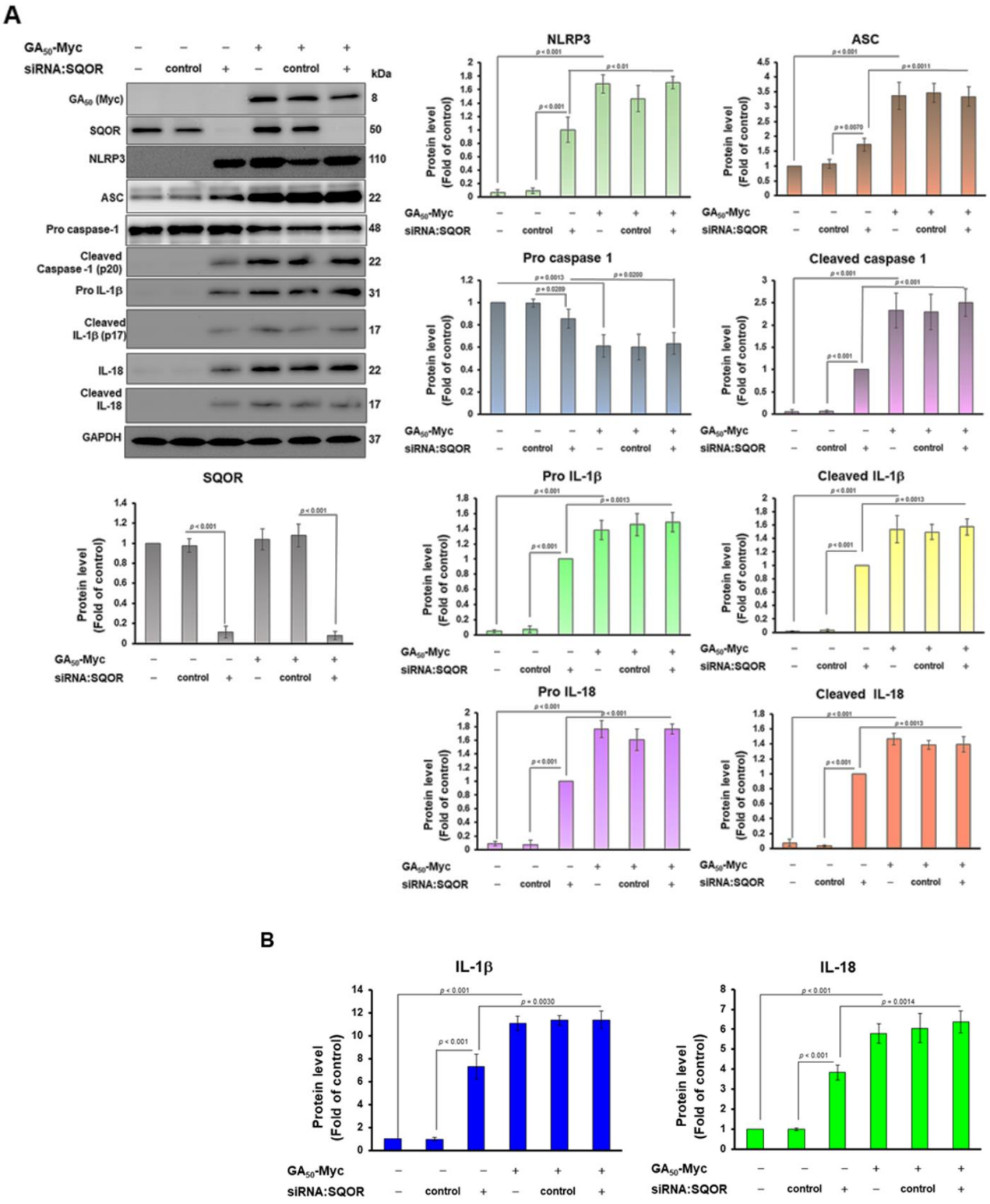

Figure 5. SQOR knockdown in HMC3 cells directly activates NLRP3 inflammasome but fails to enhance the effect of GA_{50}. We used siRNA to knockdown the expression of SQOR in non-expressing and GA50-expressing HMC3 cells for 24 h. (**A**) Cell lysates were detected by Western blot for the level of GA50, SQOR, and NLRP3 inflammasome-associated components and quantified using ImageJ software (revision 1.53). GAPDH was used as an internal loading control. (**B**) Exocrine levels of mature IL-1β and mature IL-18 in conditional media were assessed by ELISA.

As a previous experiment confirmed that SQOR knockdown can activate the NLRP3 inflammasome in HMC3 cells, we wanted to confirm whether the inhibition of SQOR expression was the main reason for GA_{50}-induced NLRP3 inflammasome activity. We treated GA_{50}-expressing HMC3 cells with *SQOR* siRNA for 24 h. Western blotting showed that the expression of SQOR in GA_{50}-expressing HMC3 cells was reduced in the *SQOR* siRNA group compared with that in the control siRNA group ($p < 0.001$, Figure 5A). While in the *SQOR* siRNA/GA_{50}-expressing group, the levels of NLRP3, ASC, cleaved caspase 1 (p20), pro IL-1β, cleaved IL-1β (p17), pro IL-18, and cleaved IL-18 were not significant changed compared to the control siRNA/GA_{50}-expressing group (Figure 5A). In addition, ELISA of conditioned media showed no significant difference in the exocrine levels of mature IL-1β and mature IL-18 in the *SQOR* siRNA/GA_{50}-expressing group compared with the control siRNA/GA_{50}-expressing group (Figure 5B). These data revealed that SQOR knockdown induced lower activity of the NLRP3 inflammasome than that caused by GA_{50} expression. SQOR knockdown did not significantly enhance GA_{50}-induced NLRP3 inflammasome activity. It is indicated that GA_{50} may activate the NLRP3 inflammasome in HMC3 cells partly by binding to inhibit SQOR activity.

3.5. GA50 Expression or SQOR Knockdown Increased ROS Generation and Cytoplasmic Escape of Mitochondrial DNA in HMC Cells

Intracellular ROS production and cytoplasmic escape of mitochondrial DNA (mtDNA) due to mitochondrial dysfunction are known to be factors that induce NLRP3 inflammasome activation [40]. SQOR is an important protein involved in the redox reaction and electron transport chain in mitochondria. SQOR deficiency causes mitochondrial dysfunction [41]. Therefore, we further analyzed the effects of SQOR knockdown and GA_{50} expression on ROS production and mtDNA cytoplasmic escape in HMC3 cells. The results showed that the downregulation of SQOR or the expression of GA_{50} significantly increased the generation of ROS ($p < 0.001$, Figure 6A) and the cytoplasmic escape of mtDNA ($p < 0.001$, Figure 6B) in HMC3 cells. The effect of GA_{50} expression on these two phenomena was stronger than that of SQOR knockdown, which is consistent with the difference in the induction of NLRP3 inflammasome activity. While in the *SQOR* siRNA/GA_{50}-expressing group, the levels of ROS had no significant changes compared to the control siRNA/GA_{50}-expressing group (Figure 6A). In addition, cytoplasmic mtDNA level showed no significant difference in the *SQOR* siRNA/GA_{50}-expressing group compared with the control siRNA/GA_{50}-expressing group (Figure 6B). These data indicated that GA_{50} may rise ROS and cytoplasmic mtDNA level in HMC3 cells partly by binding to inhibit SQOR activity.

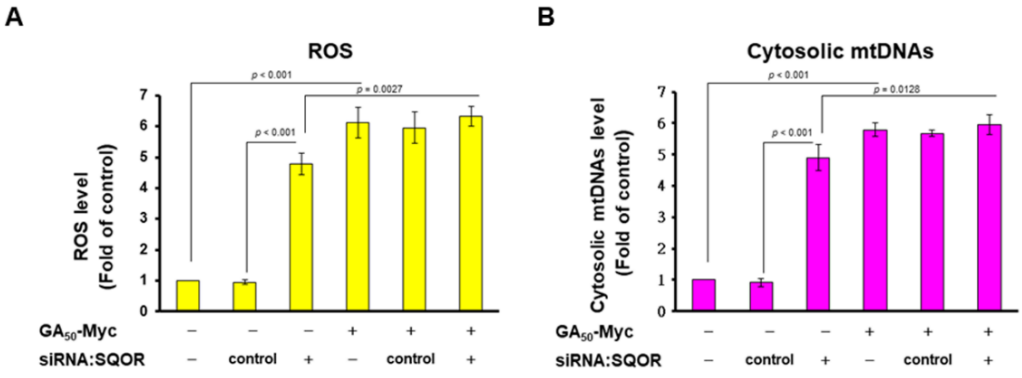

Figure 6. GA_{50} expression or SQOR knockdown increased the generation of ROS and the cytoplasmic escape of mitochondrial DNA in HMC3 cells. (**A**) ROS levels in HMC3 cells with GA_{50} expression or SQOR knockdown were measured by H2DCFDA probe and flow cytometry. (**B**) RT-qPCR was used to analyze the relative changes in the content of mitochondrial ND-1 DNA in the cytoplasm (normalized to ND-1 DNA of total lysates) to determine the degree of cytoplasmic escape of mitochondrial DNA.

3.6. The Interaction between GA50 and SQOR Can Be Inhibited by Irisflorentin in the Yeast Two-Hybrid Model

As our study found that the main reason for GA_{50} to activate the NLRP3 inflammasome of HMC3 cells is its interaction with SQOR, we hope to establish a feasible method to reverse the pathological progression of C9-ALS by disrupting the interaction between GA_{50} and SQOR, such as finding small molecule inhibitors. We used a yeast two-hybrid-based growth assay [42] to screen dozens of small chemical molecules in our laboratory (Figure 7A). Screening results revealed that irisflorentin (IFT) has this property. The results of yeast spot assay and quantification of the optical density of the yeast culture showed that the growth of BD-/AD-diploid yeast on the non-selective(SD/-Leu/-Trp) plate (or broth) was not significantly affected after IFT treatment below 100 μM. However, it failed to grow on selective (SD/-Ade/-His/-Leu/-Trp) plates (or broth) as predicted (Figure 7B,F). The growth of diploid yeast of BD-P53/AD-T in non-selective or selective culture plates (or broth) under 100 μM IFT treatment was not affected, but growth was slightly slower on selective plates (or broth) (Figure 7C,G). The above observations indicated that IFT treatment below 100 μM was not significantly toxic to yeast. Next, we found that diploid yeast of BD-GA_{50}/AD-SQOR(S3) grew unaffected on SD/-Leu/-Trp plates (broth) by 100 μM IFT treatment. However, growth in selective culture plates (or broth) showed a IFT dose-dependent decrease ($p < 0.001$, 100 μM IFT, 48 h) (Figure 7D,H). This indicates that the interaction between GA_{50} and SQOR is blocked by IFT treatment. Diploid yeast experiments with S3/AD-GA_{50} also showed the same results ($p < 0.001$, 100 μM IFT, 48 h) (Figure 7E,I).

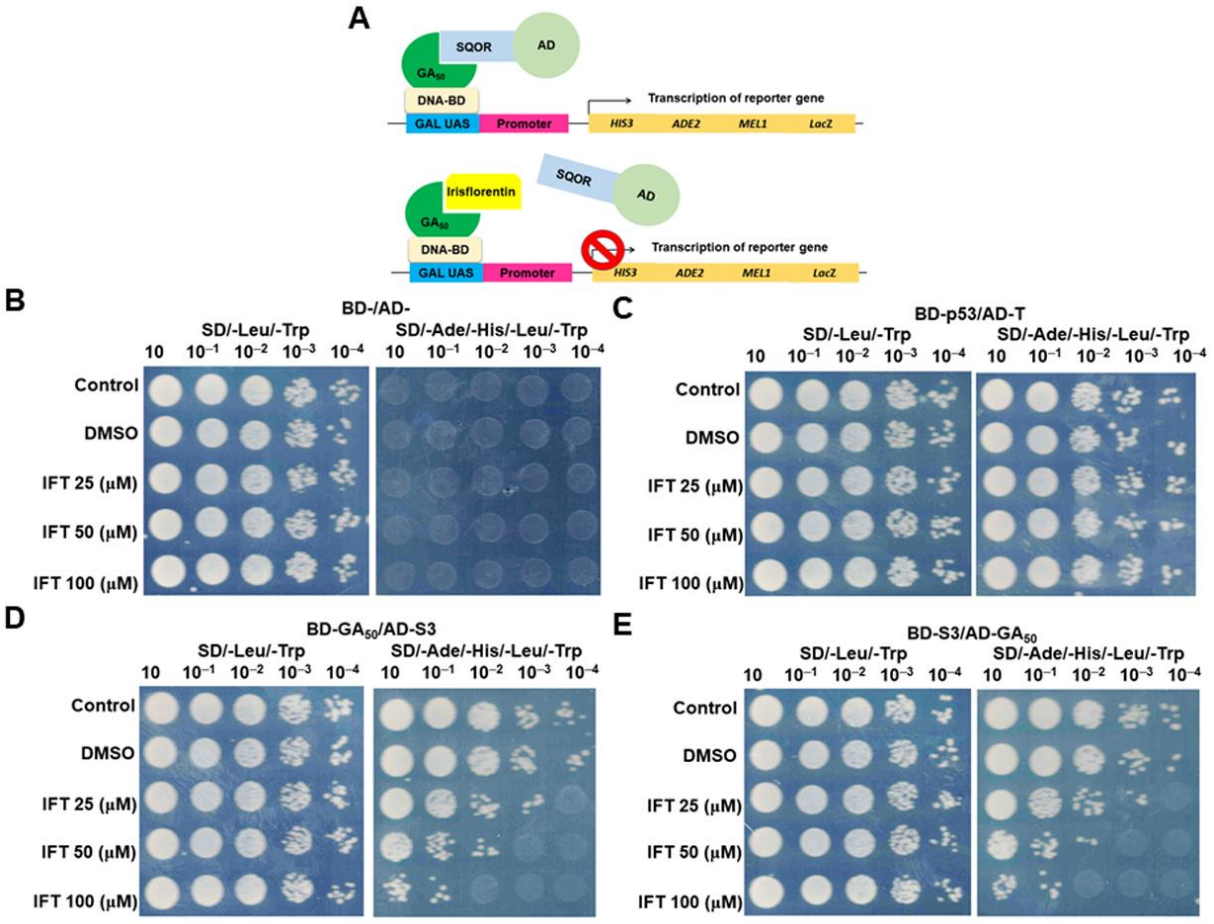

Figure 7. *Cont.*

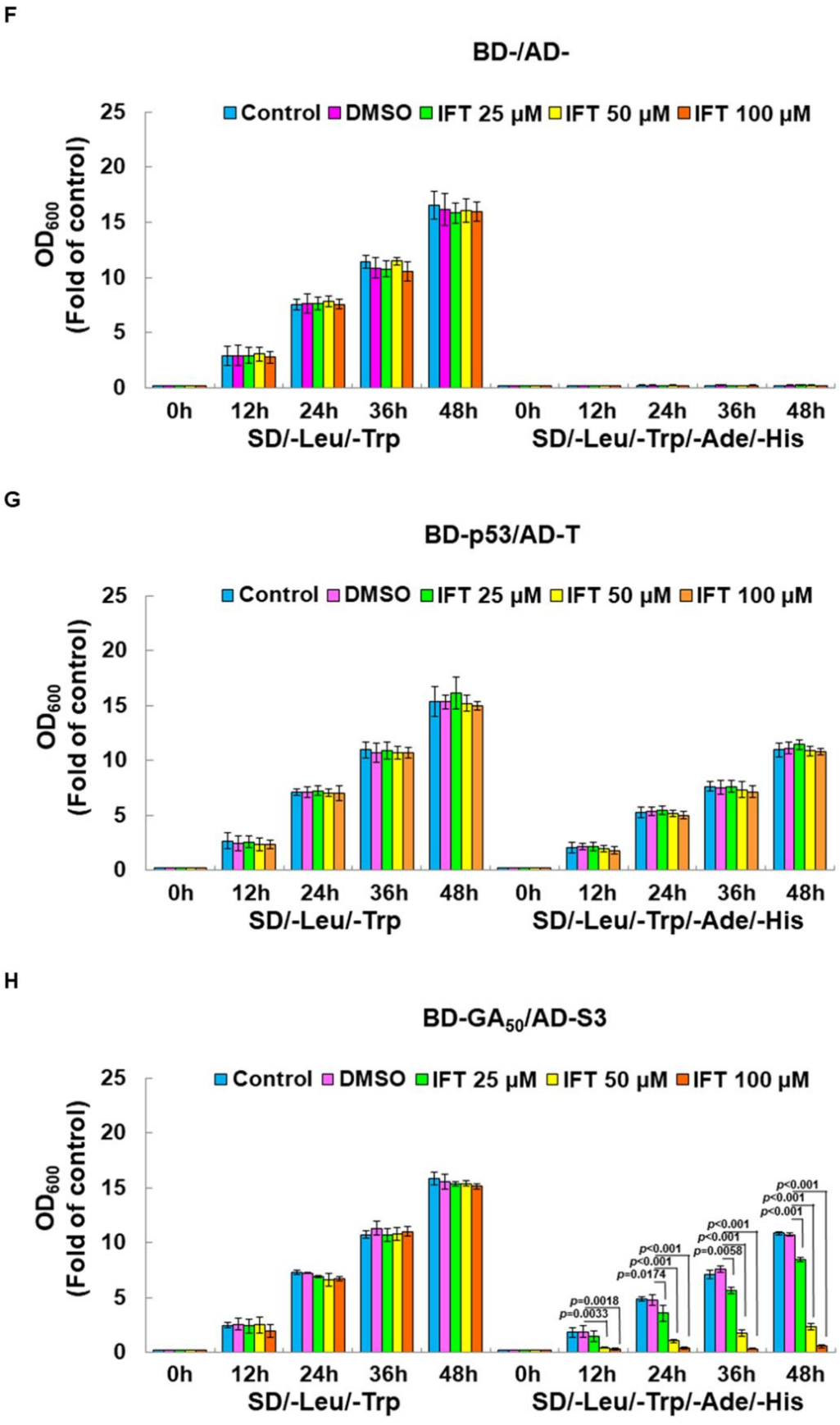

Figure 7. *Cont.*

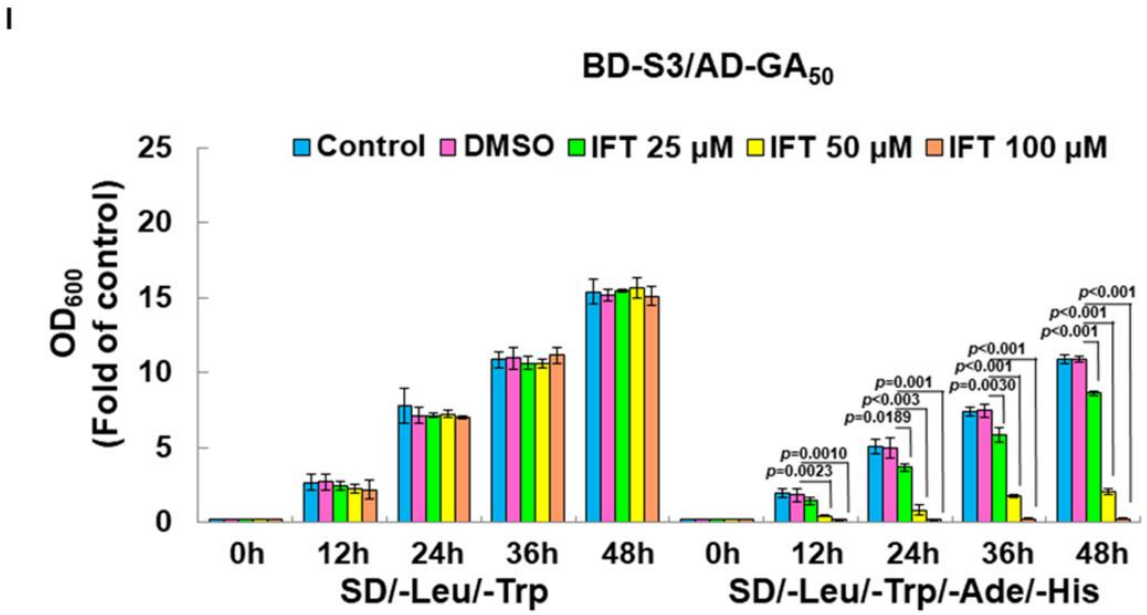

Figure 7. Irisflorentin (IFT) blocks the interaction of GA_{50} and SQOR in a yeast two-hybrid model. (**A**) Schematic showing the strategy based on the yeast two-hybrid principle to screen inhibitors of the interaction between GA_{50} and SQOR. (**B**–**I**) Diploid yeast harboring plasmids encoding BD-/AD-, BD-p53/AD-T, BD-GA_{50}/AD-SQOR (S3), or BD-S3/AD-GA_{50} grow to logarithmic phase in non-selective broth (SD/-Leu/-Trp) containing serially diluted IFT. (**B**–**E**) In yeast spot analysis, the amount of diploid yeast in each group was normalized and serially diluted, then spotted on non-selective and selective (SD/-Leu/-Trp/-Ade/-His) culture plates. Spots were incubated at 30°C for 3 days. (**F**–**I**) Diploid yeasts from each group were normalized (OD_{600} = 0.2) and cultured in non-selective and selective broth for 2 days for optical density measurements at 12 h intervals.

3.7. Irisflorentin (IFT) Reverses GA_{50}-Caused Activity of NLRP3-Inflammasome in HMC3 Cells

The previous experiment showed that IFT can block the interaction between GA_{50} and SQOR in the yeast two-hybrid model; therefore, we further assessed whether IFT can inhibit the activity of the NLRP3 inflammasome induced by GA_{50} in HMC3 cells. First, to prevent cytotoxicity from the IFT concentrations used for treatment, we performed MTT assays. The results showed that the survival of HMC3 cells was not significantly affected after 24 h of IFT treatment below 20 μM (Figure 8A). We also found that the co-immunoprecipitation interaction of GA_{50} and SQOR in 293T cells was accompanied by a concentration-dependent reduction in IFT at IFT-treated concentrations below 20 μM (Figure 8B). Moreover, GA_{50}-caused activity of the NLRP3 inflammasome in HMC3 cells was IFT concentration-dependently decreased after 24 h treatment. Quantified by Western blotting, the levels of NLRP3 ($p < 0.001$), ASC ($p < 0.001$), cleaved caspase 1 (p20) ($p < 0.001$), cleaved IL-1β (p17) ($p < 0.001$), and cleaved IL-18 ($p < 0.001$) were significantly diminished (Figure 8C). ELISA for the determination of the conditioned medium also showed that the exocrine levels of mature IL-1β ($p < 0.001$) and mature IL-18 ($p < 0.001$) in HMC3 cells expressing GA_{50}, compared with the DMSO group, in the IFT group (20 μM) were also significantly reduced ($p < 0.001$ Figure 8D). To more precisely determine that the function of IFT is to inhibit interaction of GA_{50} and SQOR rather than NLRP3 inflammasome activity, we treated HMC3 cells of SQOR-knockdown with IFT. The results revealed that the upregulated NLRP3 inflammasome activity was not significantly reduced (Figure 8E). The above data indicated that IFT could specifically reverse the activity of GA_{50}-induced NLRP3 inflammasome in microglia by blocking the interaction between GA_{50} and SQOR.

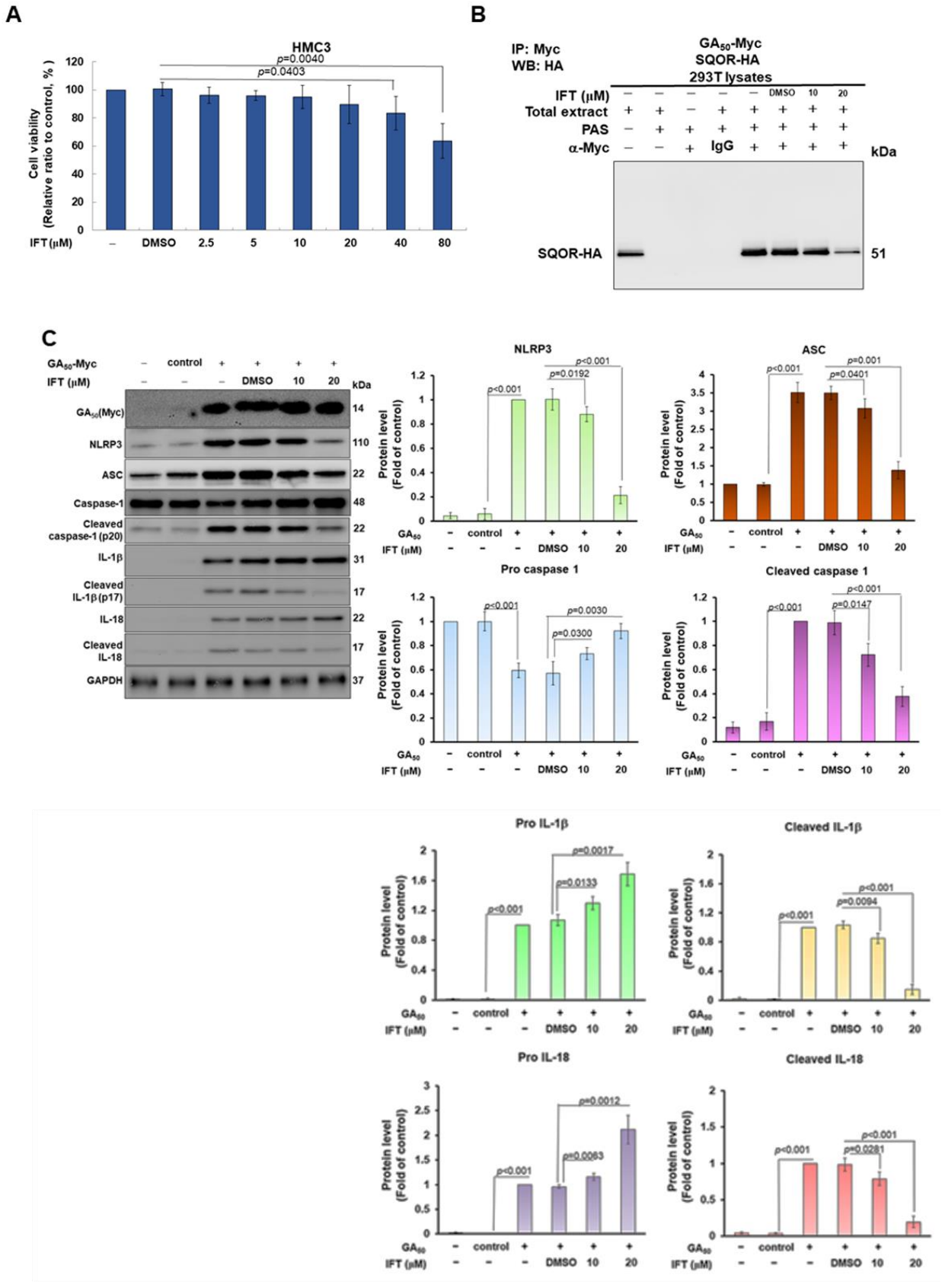

Figure 8. *Cont.*

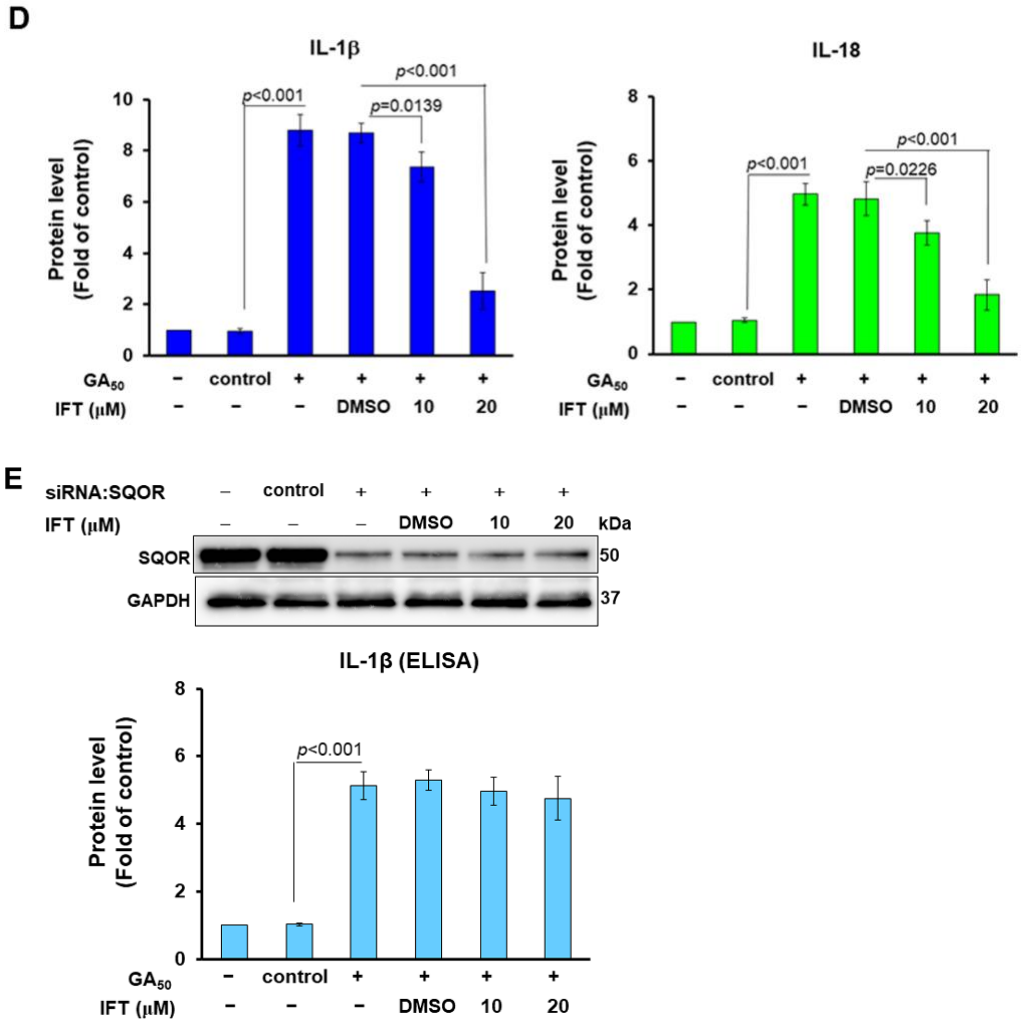

Figure 8. Irisflorentin (IFT) reverses NLRP3 inflammasome activity in GA_{50}-expressing HMC3 microglia. (**A**) Cell viability was determined by MTT assay. HMC3 cells were analyzed after treatment with DMSO, 2.5, 5, 10, 20, 40, or 80 μM IFT for 24 h. (**B**) IFT inhibits the interaction of GA_{50} and SQOR in a co-immunoprecipitation assay of 293T cells expressing GA_{50}-Myc and SQOR-HA. (**C**) Expression of GA_{50} (Myc) and NLRP3 inflammasome-associated components in cell lysates was quantified by Western blotting and ImageJ software (version 1.53). The internal loading control protein is GAPDH. (**D**) The exocrine levels of mature IL-1β and mature IL-18 in conditioned media were determined by ELISA. (**E**) Western blot analysis of the expression of SQOR and NLRP3 inflammasome-associated components in SQOR-knockdown HMC3 cells (**top** panel). GAPDH served as an internal loading control. Mature IL-1β activity in the conditional medium was detected by ELISA (**bottom** panel).

4. Discussion

C9-ALS patients have an augmented tendency to develop autoimmune diseases due to the continuous production of uncontrolled inflammatory cytokines. This indicates that *C9orf72* mutation directly or indirectly affects some inflammatory events [43]. Microglia are the most important immune cells in the brain and play an important role in maintaining the health of neurons and homeostasis of niches [44]. Activation of the NLRP3 inflammasome in microglia is known to be an important pathological factor in ALS [45]. Priming and activation are two essential steps for activating the canonical NLRP3 inflammasome [46]. Priming induces NF-κB transcriptional activity and are involved in the expression of NLRP3, IL-1β, and IL-18. Next, various factors including ROS promote NLRP3 oligomerization and recruit CARD-containing adapter protein apoptosis-associated speck-like protein (ASC), which then binds procaspase-1 to form a complex called the inflammasome. Finally, pro-

caspase-1 self-cleavage and activation convert pro-IL-1β and pro-IL-18 to active mature forms and releases them. At the same time, it also cleaves the N-terminal fragment of gasdermin-D (GSDMD) to form a cleavage hole, which promotes pyroptosis. This phase is called activation [47]. Mature IL-1β and IL-18 mediate inflammatory responses to cause damage and death of neighboring neurons [48]. Observations of ALS patients and *TDP-43* and *SOD1* mutant mice showed NLRP3 activation, increases in IL-18, and cleavages of GSDMD in microglial cells distributed in the spinal cord and motor cortex of the brain [49–51].

In this study, we found that the endogenous expression of C9-ALS associated GA-DPR (GA_{50}) induced the priming and activation of the NLRP3 inflammasome in the HMC3 human microglial cell line. MCC950 (NLRP3 inhibitor) treatment confirmed the role of GA-DPR in NLRP3 inflammasome activation. Some abnormal protein aggregation associated with neurodegenerative diseases, such as amyloid beta peptide (Aβ) in Alzheimer's disease [52], α-synuclein in Parkinson's disease [53], and SOD1 and TDP-43 [51] in ALS, are known to induce the activity of the NLRP3 inflammasome in a mouse model. Recently, Shu et al. also reported that GA-DPR can activate the NLRP3 inflammasome in mouse brain microglial cells, but they did not explore the mechanism of NLRP3 inflammasome activation. They found that aberrant NLRP3 inflammasome activity enhances ADAM10-mediated TREM2 cleavage, leading to the inhibition of GA-DPR phagocytosis [54]. In addition, we found that GA_{50} also induces apoptosis in HMC3 cells in addition to the pyroptosis induced by NLRP3 inflammasome activation. This may be because caspase-1 can activate the apoptosis process by cleaving and activating caspase-3 [55].

To explore the possible mechanism of GA-DPR activating the NLRP3 inflammasome, we used ELISA to detect GA-DPR (Myc) in the conditional medium. The results showed a weak signal, indicating that a small amount of GA-DPR was transported out of the cell and may bind to a specific receptor on the cell surface as a DAMP to induce priming of the NLRP3 inflammasome. In addition, we confirmed that GA-DPR interacts with sulfide quinone oxidoreductase (SQOR) by yeast two-hybrid screening. The interaction region is located at the C-terminal fragment of SQOR (amino acid sequence 301–450). This region contains a part of the enzyme active region. Up to now, there are no detailed reports about the function of SQOR. It may function in mitochondria to catalyze the conversion of sulfide to persulfides, thereby decreasing the toxic concentrations of sulfide [56,57]. The low level of SQOR in the brain and spinal cord in most mammals results in a limited ability to catabolize sulfide in these regions. Therefore, these regions are particularly sensitive to the toxicity of sulfide accumulation [58]. Moreover, under physiological conditions, SQOR activity promotes mitochondrial ATP synthesis. This is achieved by sulfide oxidation, which donates electrons to complex III of the mitochondrial electron transport chain (ETC) via coenzyme Q (CoQ), or by generating persulfides that can serve as electron acceptors of ETC [59]. The study showed that increasing the expression of SQOR improves ischemic brain injury [58]. Furthermore, the downregulation of SQOR in HeLa cells increased ROS in the cells [60]. Studies have shown that oxidative stress disrupts the mitochondrial membrane potential, leading to depolarization. In addition to affecting the normal function of mitochondria, depolarization can also induce the opening of mitochondrial permeability transition pore (MPTP), which allows the release of mitochondrial ROS (mtROS), DNA (mtDNA), or intermembrane space proteins into the cytoplasm [61]. Both mtROS and mtDNA are active factors that induce NLRP3 inflammasome [39]. In particular, cytosolic, oxidized mtDNA can activate the inflammasome by binding to the inflammasome sensors AIM2 and NL RP3 [62].

As the relationship between SQOR and NLRP3 inflammasome is not clear, we use siRNA to down-regulate SQOR in microglial cells to measure the change in NLRP3 inflammasome activity. The results showed that SQOR knockdown could induce NLRP3 inflammasome activity as significantly as GA-DPR expression. Moreover, we found that both GA_{50} expression and SQOR knockdown in HMC3 cells significantly induced ROS production and cytoplasmic mtDNA escape. However, HMC3 cells with GA_{50} expression and SQOR downregulation did not enhance NLRP3 inflammasome activity compared with GA_{50}-expressing cells. According

to the above results, the expression of GA_{50} in microglial cells may partly cause the increase in mitochondrial ROS and the cytoplasmic escape of mtDNA through the inhibition of SQOR activity, thereby activating the NLRP3 inflammasome.

Another possible effect of GA_{50} on the inhibition of SQOR function is the accumulation of SQOR substrates hydrogen sulfide (H_2S) in cells [59]. H_2S is an environmental toxin and an endogenous gasotransmitter (or neurotransmitter). It is an essential molecule that not only acts as a vasodilator, cytoprotectant, antioxidant, and anti-inflammatory agent but also acts as a poison [63]. It is generally believed that H_2S has beneficial effects at physiological concentrations (nM to low-μM) but may lead to harmful effects at higher concentrations [64]. A study showed high H_2S levels in the cerebrospinal fluid and nerve tissue of SOD1 mutant ALS mice and sporadic ALS patients [65]. This H_2S mainly comes from glial cells [65]. In addition, the study found that a higher H_2S concentration increases the intracellular calcium ion concentration of motor neurons, inhibits mitochondrial respiration, and reduces ATP production. Higher H_2S levels also enhance pathways related to oxidative stress and cell death [65]. In the analysis of the NLRP3 inflammasome in microglial cells, some studies have shown that H_2S treatment can inhibit the activity of the NLRP3 inflammasome [66,67]. However, some studies have also shown that H2S exposure can induce the secretion of NLRP3 inflammasome-dependent IL-1β and IL-18 in human mononuclear leukocytes [68] and broiler thymocytes [69]. This effect may be because H_2S activates the NLRP3 inflammasome through the TLR-7/MyD 88/NF-κB pathway [69]. These differential effects on NLRP3 inflammasome activity may be related to the concentration of H_2S treatment, cell types, or animal models. Although we did not measure the amount of H2S in HMC3 cells with or without expression of GA_{50} in this study, we confirmed that part of the active region of the SQOR enzyme was bound by GA_{50} and blocked, so it is likely to increase the amount of H_2S in HMC3 cells to the level of toxicity and induce NLRP3 inflammasome activity.

Finally, we found that irisflorentin (IFT) can inhibit the interaction between GA_{50} and SQOR by using yeast two-hybrid-based growth assay and co-immunoprecipitation technique. Likewise, IFT treatment reduced GA_{50}-induced NLRP3 inflammasome activity. However, irisflorentin could not inhibit the activation of NLRP3 inflammasome caused by the downregulation of SQOR. It was confirmed that IFT specifically inhibited the interaction between GA50 and SQOR to prevent the activation of the NLRP3 inflammasome. IFT is isolated from the root of *Belamcanda chinensis* (L.) DC, which has various biological activities. [70]. Studies have shown that IFT can enhance the expression of antioxidant enzymes and improve keratinocyte apoptosis and collagen degradation caused by ultraviolet-B-induced ROS [71]. IFT has also been shown to ameliorate 6-OHDA-induced dopaminergic neuronal degeneration and α-synuclein accumulation in Parkinson's disease models [72]. Moreover, IFT can inhibit allergic contact hypersensitivity by modifying the properties of mouse bone marrow dendritic cells [73] and can improve the LPS-induced inflammatory response of RAW 264.7 macrophages [74]. Therefore, in addition to diminishing the activity of the NLRP3 inflammasome induced by GA_{50}, IFT may also have neuroprotective activities in regulating cellular anti-oxidation, anti-inflammation, and clearing amyloid in C9-ALS patients. Several studies have shown that the inhibitor of the NLRP3 inflammasome (MCC950) can effectively reverse the motor deficits in ALS-containing GA-DPR-expressing mice caused by the activation of the NLRP3 inflammasome [54]. However, this non-specific broad inhibition of NLRP3 inflammasome activity may disrupt innate immune mechanisms and increase the chances of infection in patients. Therefore, for C9-ALS, the therapeutic strategy of IFT can avoid this risk.

Taken together, the results of this study provide a novel explanation for the establishment of C9-ALS. GA-DPR may cause the generation of ROS and cytoplasmic escape of mtDNA in microglial cells by binding and regulating the activity of SQOR. Finally, the activation of the NLRP3 inflammasome affects the survival and function of surrounding neurons. In addition, we found that IFT is a specific inhibitor of this abnormal interaction and has the potential to be developed as an anti-C9-ALS drug.

Author Contributions: Conceptualization, R.-H.F.; methodology, R.-H.F. and H.-J.C.; validation, R.-H.F.; investigation, R.-H.F., H.-J.C. and S.-Y.H.; resources, R.-H.F. and H.-J.C.; writing—original draft, R.-H.F.; writing—review and editing, R.-H.F.; visualization, R.-H.F.; supervision, R.-H.F.; project administration, R.-H.F.; Funding acquisition, R.-H.F. All authors have read and agreed to the published version of the manuscript.

Funding: This research was funded in part by the Ministry of Science and Technology (Taiwan), MOST 105-2314-B-039-017-MY3, and China Medical University Hospital (Taiwan), DMR-111-140.

Institutional Review Board Statement: Not applicable.

Informed Consent Statement: Not applicable.

Data Availability Statement: The data presented in this study are available on request from the corresponding author.

Acknowledgments: We are thankful to Silvia Chan for her editing service.

Conflicts of Interest: The authors declare no conflict of interest.

References

1. Mehta, P.; Raymond, J.; Punjani, R.; Han, M.; Larson, T.; Kaye, W.; Nelson, L.M.; Topol, B.; Muravov, O.; Genson, C.; et al. Prevalence of amyotrophic lateral sclerosis in the United States using established and novel methodologies, 2017. *Amyotroph Lateral Scler Front. Degener* **2022**, *24*, 108–116. [CrossRef] [PubMed]
2. Mitsumoto, H.; Brooks, B.R.; Silani, V. Clinical trials in amyotrophic lateral sclerosis: Why so many negative trials and how can trials be improved? *Lancet. Neurol.* **2014**, *13*, 1127–1138. [CrossRef] [PubMed]
3. Paez-Colasante, X.; Figueroa-Romero, C.; Sakowski, S.A.; Goutman, S.A.; Feldman, E.L. Amyotrophic lateral sclerosis: Mechanisms and therapeutics in the epigenomic era. *Nat. Rev. Neurol.* **2015**, *11*, 266–279. [CrossRef]
4. Peters, O.M.; Ghasemi, M.; Brown, R.H., Jr. Emerging mechanisms of molecular pathology in ALS. *J. Clin. Investig.* **2015**, *125*, 1767–1779. [CrossRef]
5. Rohrer, J.D.; Isaacs, A.M.; Mizielinska, S.; Mead, S.; Lashley, T.; Wray, S.; Sidle, K.; Fratta, P.; Orrell, R.W.; Hardy, J.; et al. C9orf72 expansions in frontotemporal dementia and amyotrophic lateral sclerosis. *Lancet Neurol.* **2015**, *14*, 291–301. [CrossRef]
6. Prudencio, M.; Belzil, V.V.; Batra, R.; Ross, C.A.; Gendron, T.F.; Pregent, L.J.; Murray, M.E.; Overstreet, K.K.; Piazza-Johnston, A.E.; Desaro, P.; et al. Distinct brain transcriptome profiles in C9orf72-associated and sporadic ALS. *Nat. Neurosci.* **2015**, *18*, 1175–1182. [CrossRef] [PubMed]
7. Suzuki, N.; Maroof, A.M.; Merkle, F.T.; Koszka, K.; Intoh, A.; Armstrong, I.; Moccia, R.; Davis-Dusenbery, B.N.; Eggan, K. The mouse C9ORF72 ortholog is enriched in neurons known to degenerate in ALS and FTD. *Nat. Neurosci.* **2013**, *16*, 1725–1727. [CrossRef]
8. Mackenzie, I.R.; Frick, P.; Neumann, M. The neuropathology associated with repeat expansions in the C9ORF72 gene. *Acta Neuropathol.* **2014**, *127*, 347–357. [CrossRef]
9. Woollacott, I.O.; Mead, S. The C9ORF72 expansion mutation: Gene structure, phenotypic and diagnostic issues. *Acta Neuropathol.* **2014**, *127*, 319–332. [CrossRef]
10. Cooper-Knock, J.; Shaw, P.J.; Kirby, J. The widening spectrum of C9ORF72-related disease; genotype/phenotype correlations and potential modifiers of clinical phenotype. *Acta Neuropathol.* **2014**, *127*, 333–345. [CrossRef]
11. Gendron, T.F.; Belzil, V.V.; Zhang, Y.J.; Petrucelli, L. Mechanisms of toxicity in C9FTLD/ALS. *Acta Neuropathol.* **2014**, *127*, 359–376. [CrossRef]
12. Atkinson, R.A.; Fernandez-Martos, C.M.; Atkin, J.D.; Vickers, J.C.; King, A.E. C9ORF72 expression and cellular localization over mouse development. *Acta Neuropathol. Commun.* **2015**, *3*, 59. [CrossRef]
13. Farg, M.A.; Sundaramoorthy, V.; Sultana, J.M.; Yang, S.; Atkinson, R.A.; Levina, V.; Halloran, M.A.; Gleeson, P.A.; Blair, I.P.; Soo, K.Y.; et al. C9ORF72, implicated in amytrophic lateral sclerosis and frontotemporal dementia, regulates endosomal trafficking. *Hum. Mol. Genet.* **2014**, *23*, 3579–3595. [CrossRef]
14. Smeyers, J.; Banchi, E.G.; Latouche, M. C9ORF72: What It Is, What It Does, and Why It Matters. *Front. Cell Neurosci.* **2021**, *15*, 661447. [CrossRef] [PubMed]
15. Zheng, W.; Wang, K.; Wu, Y.; Yan, G.; Zhang, C.; Li, Z.; Wang, L.; Chen, S. C9orf72 regulates the unfolded protein response and stress granule formation by interacting with eIF2alpha. *Theranostics* **2022**, *12*, 7289–7306. [CrossRef]
16. Liu, X.; Zhao, X.; He, J.; Wang, S.; Shen, X.; Liu, Q.; Wang, S. Advances in the Structure of GGGGCC Repeat RNA Sequence and Its Interaction with Small Molecules and Protein Partners. *Molecules* **2023**, *28*, 5801. [CrossRef] [PubMed]
17. Cheng, W.; Wang, S.; Mestre, A.A.; Fu, C.; Makarem, A.; Xian, F.; Hayes, L.R.; Lopez-Gonzalez, R.; Drenner, K.; Jiang, J.; et al. C9ORF72 GGGGCC repeat-associated non-AUG translation is upregulated by stress through eIF2alpha phosphorylation. *Nat. Commun.* **2018**, *9*, 51. [CrossRef]
18. Gao, F.B.; Richter, J.D.; Cleveland, D.W. Rethinking Unconventional Translation in Neurodegeneration. *Cell* **2017**, *171*, 994–1000. [CrossRef]

19. Green, K.M.; Glineburg, M.R.; Kearse, M.G.; Flores, B.N.; Linsalata, A.E.; Fedak, S.J.; Goldstrohm, A.C.; Barmada, S.J.; Todd, P.K. RAN translation at C9orf72-associated repeat expansions is selectively enhanced by the integrated stress response. *Nat. Commun.* **2017**, *8*, 2005. [CrossRef]
20. Sonobe, Y.; Ghadge, G.; Masaki, K.; Sendoel, A.; Fuchs, E.; Roos, R.P. Translation of dipeptide repeat proteins from the C9ORF72 expanded repeat is associated with cellular stress. *Neurobiol. Dis.* **2018**, *116*, 155–165. [CrossRef] [PubMed]
21. Schmitz, A.; Pinheiro Marques, J.; Oertig, I.; Maharjan, N.; Saxena, S. Emerging Perspectives on Dipeptide Repeat Proteins in C9ORF72 ALS/FTD. *Front. Cell Neurosci.* **2021**, *15*, 637548. [CrossRef]
22. Jensen, B.K.; Schuldi, M.H.; McAvoy, K.; Russell, K.A.; Boehringer, A.; Curran, B.M.; Krishnamurthy, K.; Wen, X.; Westergard, T.; Ma, L.; et al. Synaptic dysfunction induced by glycine-alanine dipeptides in C9orf72-ALS/FTD is rescued by SV2 replenishment. *EMBO Mol. Med.* **2020**, *12*, e10722. [CrossRef] [PubMed]
23. Schludi, M.H.; May, S.; Grasser, F.A.; Rentzsch, K.; Kremmer, E.; Kupper, C.; Klopstock, T.; German Consortium for Frontotemporal Lobar, D.; Bavarian Brain Banking, A.; Arzberger, T.; et al. Distribution of dipeptide repeat proteins in cellular models and C9orf72 mutation cases suggests link to transcriptional silencing. *Acta Neuropathol.* **2015**, *130*, 537–555. [CrossRef] [PubMed]
24. Yamakawa, M.; Ito, D.; Honda, T.; Kubo, K.; Noda, M.; Nakajima, K.; Suzuki, N. Characterization of the dipeptide repeat protein in the molecular pathogenesis of c9FTD/ALS. *Hum. Mol. Genet.* **2015**, *24*, 1630–1645. [CrossRef]
25. Zhang, Y.J.; Jansen-West, K.; Xu, Y.F.; Gendron, T.F.; Bieniek, K.F.; Lin, W.L.; Sasaguri, H.; Caulfield, T.; Hubbard, J.; Daughrity, L.; et al. Aggregation-prone c9FTD/ALS poly(GA) RAN-translated proteins cause neurotoxicity by inducing ER stress. *Acta Neuropathol.* **2014**, *128*, 505–524. [CrossRef]
26. Chien, H.M.; He, R.Y.; Lee, C.C.; Huang, Y.A.; Hung, I.J.; Hou, K.T.; Hsiao, J.C.; Lu, P.C.; Agnihotri, D.; Hwang, E.; et al. Nanoscopic investigation of C9orf72 poly-GA oligomers on nuclear membrane disruption by a photoinducible platform. *Commun. Chem.* **2021**, *4*, 111. [CrossRef] [PubMed]
27. Lee, Y.B.; Baskaran, P.; Gomez, J.; Chen, H.J.; Nishimura, A.; Smith, B.; Troakes, C.; Adachi, Y.; Stepto, A.; Petrucelli, L.; et al. C9orf72 poly GA RAN-translated protein plays a key role in Amyotrophic Lateral Sclerosis via aggregation and toxicity. *Hum. Mol. Genet.* **2017**, *26*, 4765–4777. [CrossRef] [PubMed]
28. Nonaka, T.; Masuda-Suzukake, M.; Hosokawa, M.; Shimozawa, A.; Hirai, S.; Okado, H.; Hasegawa, M. C9ORF72 dipeptide repeat poly-GA inclusions promote: Intracellular aggregation of phosphorylated TDP-43. *Hum. Mol. Genet.* **2018**, *27*, 2658–2660. [CrossRef]
29. May, S.; Hornburg, D.; Schludi, M.H.; Arzberger, T.; Rentzsch, K.; Schwenk, B.M.; Grasser, F.A.; Mori, K.; Kremmer, E.; Banzhaf-Strathmann, J.; et al. C9orf72 FTLD/ALS-associated Gly-Ala dipeptide repeat proteins cause neuronal toxicity and Unc119 sequestration. *Acta Neuropathol.* **2014**, *128*, 485–503. [CrossRef]
30. Sonobe, Y.; Aburas, J.; Krishnan, G.; Fleming, A.C.; Ghadge, G.; Islam, P.; Warren, E.C.; Gu, Y.; Kankel, M.W.; Brown, A.E.X.; et al. elegans model of C9orf72-associated ALS/FTD uncovers a conserved role for eIF2D in RAN translation. *Nat. Commun.* **2021**, *12*, 6025. [CrossRef]
31. Masrori, P.; Beckers, J.; Gossye, H.; Van Damme, P. The role of inflammation in neurodegeneration: Novel insights into the role of the immune system in C9orf72 HRE-mediated ALS/FTD. *Mol. Neurodegener.* **2022**, *17*, 22. [CrossRef] [PubMed]
32. McCauley, M.E.; O'Rourke, J.G.; Yanez, A.; Markman, J.L.; Ho, R.; Wang, X.; Chen, S.; Lall, D.; Jin, M.; Muhammad, A.; et al. C9orf72 in myeloid cells suppresses STING-induced inflammation. *Nature* **2020**, *585*, 96–101. [CrossRef]
33. Pinilla, G.; Kumar, A.; Floaters, M.K.; Pardo, C.A.; Rothstein, J.; Ilieva, H. Increased synthesis of pro-inflammatory cytokines in C9ORF72 patients. *Amyotroph. Lateral Scler. Front. Degener.* **2021**, *22*, 517–527. [CrossRef] [PubMed]
34. Wang, M.J.; Kang, L.; Wang, Y.Z.; Yang, B.R.; Zhang, C.; Lu, Y.F.; Kang, L. Microglia in motor neuron disease: Signaling evidence from last 10 years. *Dev. Neurobiol.* **2022**, *82*, 625–638. [CrossRef] [PubMed]
35. LaClair, K.D.; Zhou, Q.; Michaelsen, M.; Wefers, B.; Brill, M.S.; Janjic, A.; Rathkolb, B.; Farny, D.; Cygan, M.; de Angelis, M.H.; et al. Congenic expression of poly-GA but not poly-PR in mice triggers selective neuron loss and interferon responses found in C9orf72 ALS. *Acta Neuropathol.* **2020**, *140*, 121–142. [CrossRef]
36. Zhang, H.; Li, H.; Huang, B.; Wang, S.; Gao, Y.; Meng, F.; Chen, Y.; Zhou, F.; Guan, Y.; Wang, X. Spatiotemporal evolution of pyroptosis and canonical inflammasome pathway in hSOD1(G93A) ALS mouse model. *BMC Neurosci.* **2022**, *23*, 50. [CrossRef] [PubMed]
37. Clenet, M.L.; Keaney, J.; Gillet, G.; Valadas, J.S.; Langlois, J.; Cardenas, A.; Gasser, J.; Kadiu, I. Divergent functional outcomes of NLRP3 blockade downstream of multi-inflammasome activation: Therapeutic implications for ALS. *Front. Immunol.* **2023**, *14*, 1190219. [CrossRef]
38. Fu, R.H.; Tsai, C.W.; Chiu, S.C.; Liu, S.P.; Chiang, Y.T.; Kuo, Y.H.; Shyu, W.C.; Lin, S.Z. C9-ALS-Associated Proline-Arginine Dipeptide Repeat Protein Induces Activation of NLRP3 Inflammasome of HMC3 Microglia Cells by Binding of Complement Component 1 Q Subcomponent-Binding Protein (C1QBP), and Syringin Prevents This Effect. *Cells* **2022**, *11*, 3128. [CrossRef]
39. Zhang, W.; Li, G.; Luo, R.; Lei, J.; Song, Y.; Wang, B.; Ma, L.; Liao, Z.; Ke, W.; Liu, H.; et al. Cytosolic escape of mitochondrial DNA triggers cGAS-STING-NLRP3 axis-dependent nucleus pulposus cell pyroptosis. *Exp. Mol. Med.* **2022**, *54*, 129–142. [CrossRef]
40. Zhao, Y.; Liu, B.; Xu, L.; Yu, S.; Fu, J.; Wang, J.; Yan, X.; Su, J. ROS-Induced mtDNA Release: The Emerging Messenger for Communication between Neurons and Innate Immune Cells during Neurodegenerative Disorder Progression. *Antioxidants* **2021**, *10*, 1917. [CrossRef]

41. Kumar, R.; Landry, A.P.; Guha, A.; Vitvitsky, V.; Lee, H.J.; Seike, K.; Reddy, P.; Lyssiotis, C.A.; Banerjee, R. A redox cycle with complex II prioritizes sulfide quinone oxidoreductase-dependent H(2)S oxidation. *J. Biol. Chem.* **2022**, *298*, 101435. [CrossRef]
42. Wong, J.H.; Alfatah, M.; Sin, M.F.; Sim, H.M.; Verma, C.S.; Lane, D.P.; Arumugam, P. A yeast two-hybrid system for the screening and characterization of small-molecule inhibitors of protein-protein interactions identifies a novel putative Mdm2-binding site in p53. *BMC Biol.* **2017**, *15*, 108. [CrossRef]
43. Pang, W.; Hu, F. C9ORF72 suppresses JAK-STAT mediated inflammation. *iScience* **2023**, *26*, 106579. [CrossRef]
44. Lorenzini, I.; Alsop, E.; Levy, J.; Gittings, L.M.; Lall, D.; Rabichow, B.E.; Moore, S.; Pevey, R.; Bustos, L.M.; Burciu, C.; et al. Moderate intrinsic phenotypic alterations in C9orf72 ALS/FTD iPSC-microglia despite the presence of C9orf72 pathological features. *Front. Cell Neurosci.* **2023**, *17*, 1179796. [CrossRef] [PubMed]
45. Trageser, K.J.; Yang, E.J.; Smith, C.; Iban-Arias, R.; Oguchi, T.; Sebastian-Valverde, M.; Iqbal, U.H.; Wu, H.; Estill, M.; Al Rahim, M.; et al. Inflammasome-Mediated Neuronal-Microglial Crosstalk: A Therapeutic Substrate for the Familial C9orf72 Variant of Frontotemporal Dementia/Amyotrophic Lateral Sclerosis. *Mol. Neurobiol.* **2023**, *60*, 4004–4016. [CrossRef] [PubMed]
46. Swanson, K.V.; Deng, M.; Ting, J.P. The NLRP3 inflammasome: Molecular activation and regulation to therapeutics. *Nat. Rev. Immunol.* **2019**, *19*, 477–489. [CrossRef]
47. Munoz-Planillo, R.; Kuffa, P.; Martinez-Colon, G.; Smith, B.L.; Rajendiran, T.M.; Nunez, G. K(+) efflux is the common trigger of NLRP3 inflammasome activation by bacterial toxins and particulate matter. *Immunity* **2013**, *38*, 1142–1153. [CrossRef] [PubMed]
48. Wang, H.; Shi, X.; Qiu, M.; Lv, S.; Zheng, H.; Niu, B.; Liu, H. Hydrogen Sulfide Plays an Important Role by Influencing NLRP3 inflammasome. *Int. J. Biol. Sci.* **2020**, *16*, 2752–2760. [CrossRef]
49. Chiarini, A.; Gui, L.; Viviani, C.; Armato, U.; Dal Pra, I. NLRP3 Inflammasome's Activation in Acute and Chronic Brain Diseases-An Update on Pathogenetic Mechanisms and Therapeutic Perspectives with Respect to Other Inflammasomes. *Biomedicines* **2023**, *11*, 999. [CrossRef]
50. Van Schoor, E.; Ospitalieri, S.; Moonen, S.; Tome, S.O.; Ronisz, A.; Ok, O.; Weishaupt, J.; Ludolph, A.C.; Van Damme, P.; Van Den Bosch, L.; et al. Increased pyroptosis activation in white matter microglia is associated with neuronal loss in ALS motor cortex. *Acta Neuropathol.* **2022**, *144*, 393–411. [CrossRef]
51. Deora, V.; Lee, J.D.; Albornoz, E.A.; McAlary, L.; Jagaraj, C.J.; Robertson, A.A.B.; Atkin, J.D.; Cooper, M.A.; Schroder, K.; Yerbury, J.J.; et al. The microglial NLRP3 inflammasome is activated by amyotrophic lateral sclerosis proteins. *Glia* **2020**, *68*, 407–421. [CrossRef]
52. Van Zeller, M.; Dias, D.; Sebastiao, A.M.; Valente, C.A. NLRP3 Inflammasome: A Starring Role in Amyloid-beta- and Tau-Driven Pathological Events in Alzheimer's Disease. *J. Alzheimers Dis.* **2021**, *83*, 939–961. [CrossRef]
53. Han, Q.Q.; Le, W. NLRP3 Inflammasome-Mediated Neuroinflammation and Related Mitochondrial Impairment in Parkinson's Disease. *Neurosci. Bull.* **2023**, *39*, 832–844. [CrossRef]
54. Shu, X.; Wei, C.; Tu, W.Y.; Zhong, K.; Qi, S.; Wang, A.; Bai, L.; Zhang, S.X.; Luo, B.; Xu, Z.Z.; et al. Negative regulation of TREM2-mediated C9orf72 poly-GA clearance by the NLRP3 inflammasome. *Cell Rep.* **2023**, *42*, 112133. [CrossRef] [PubMed]
55. Fink, S.L.; Cookson, B.T. Caspase-1-dependent pore formation during pyroptosis leads to osmotic lysis of infected host macrophages. *Cell Microbiol.* **2006**, *8*, 1812–1825. [CrossRef] [PubMed]
56. Ackermann, M.; Kubitza, M.; Maier, K.; Brawanski, A.; Hauska, G.; Pina, A.L. The vertebrate homolog of sulfide-quinone reductase is expressed in mitochondria of neuronal tissues. *Neuroscience* **2011**, *199*, 1–12. [CrossRef]
57. Landry, A.P.; Ballou, D.P.; Banerjee, R. H2S oxidation by nanodisc-embedded human sulfide quinone oxidoreductase. *J. Biol. Chem.* **2017**, *292*, 11641–11649. [CrossRef]
58. Marutani, E.; Morita, M.; Hirai, S.; Kai, S.; Grange, R.M.H.; Miyazaki, Y.; Nagashima, F.; Traeger, L.; Magliocca, A.; Ida, T.; et al. Sulfide catabolism ameliorates hypoxic brain injury. *Nat. Commun.* **2021**, *12*, 3108. [CrossRef]
59. Landry, A.P.; Ballou, D.P.; Banerjee, R. Hydrogen Sulfide Oxidation by Sulfide Quinone Oxidoreductase. *Chembiochem* **2021**, *22*, 949–960. [CrossRef] [PubMed]
60. Kleiner, G.; Barca, E.; Ziosi, M.; Emmanuele, V.; Xu, Y.; Hidalgo-Gutierrez, A.; Qiao, C.; Tadesse, S.; Area-Gomez, E.; Lopez, L.C.; et al. CoQ(10) supplementation rescues nephrotic syndrome through normalization of H(2)S oxidation pathway. *Biochim. Biophys. Acta Mol. Basis Dis.* **2018**, *1864*, 3708–3722. [CrossRef]
61. Rottenberg, H.; Hoek, J.B. The path from mitochondrial ROS to aging runs through the mitochondrial permeability transition pore. *Aging Cell* **2017**, *16*, 943–955. [CrossRef]
62. Lawrence, G.; Holley, C.L.; Schroder, K. Come on mtDNA, light my fire. *Immunity* **2022**, *55*, 1331–1333. [CrossRef] [PubMed]
63. Vo, T.T.T.; Huynh, T.D.; Wang, C.S.; Lai, K.H.; Lin, Z.C.; Lin, W.N.; Chen, Y.L.; Peng, T.Y.; Wu, H.C.; Lee, I.T. The Potential Implications of Hydrogen Sulfide in Aging and Age-Related Diseases through the Lens of Mitohormesis. *Antioxidants* **2022**, *11*, 1619. [CrossRef]
64. Ji, Y.; Li, Y.; Zhao, Z.; Li, P.; Xie, Y. Hydrogen Sulfide Overproduction Is Involved in Acute Ischemic Cerebral Injury Under Hyperhomocysteinemia. *Front. Neurosci.* **2020**, *14*, 582851. [CrossRef] [PubMed]
65. Davoli, A.; Greco, V.; Spalloni, A.; Guatteo, E.; Neri, C.; Rizzo, G.R.; Cordella, A.; Romigi, A.; Cortese, C.; Bernardini, S.; et al. Evidence of hydrogen sulfide involvement in amyotrophic lateral sclerosis. *Ann. Neurol.* **2015**, *77*, 697–709. [CrossRef] [PubMed]
66. Bai, L.; Dai, J.; Xia, Y.; He, K.; Xue, H.; Guo, Q.; Tian, D.; Xiao, L.; Zhang, X.; Teng, X.; et al. Hydrogen Sulfide Ameliorated High Choline-Induced Cardiac Dysfunction by Inhibiting cGAS-STING-NLRP3 Inflammasome Pathway. *Oxid. Med. Cell Longev.* **2022**, *2022*, 1392896. [CrossRef]

67. Gong, W.; Zhang, S.; Chen, Y.; Shen, J.; Zheng, Y.; Liu, X.; Zhu, M.; Meng, G. Protective role of hydrogen sulfide against diabetic cardiomyopathy via alleviating necroptosis. *Free Radic. Biol. Med.* **2022**, *181*, 29–42. [CrossRef]
68. Basic, A.; Alizadehgharib, S.; Dahlen, G.; Dahlgren, U. Hydrogen sulfide exposure induces NLRP3 inflammasome-dependent IL-1beta and IL-18 secretion in human mononuclear leukocytes in vitro. *Clin. Exp. Dent. Res.* **2017**, *3*, 115–120. [CrossRef]
69. Hu, X.; Chi, Q.; Liu, Q.; Wang, D.; Zhang, Y.; Li, S. Atmospheric H2S triggers immune damage by activating the TLR-7/MyD88/NF-kappaB pathway and NLRP3 inflammasome in broiler thymus. *Chemosphere* **2019**, *237*, 124427. [CrossRef]
70. Zhang, X.; Qiao, G.X.; Zhao, G.F.; Zhao, S.F. Characterization of the metabolites of irisflorentin by using ultra-high performance liquid chromatography combined with quadrupole/orbitrap tandem mass spectrometry. *J. Pharm. Biomed. Anal.* **2021**, *203*, 114222. [CrossRef]
71. Noh, D.; Choi, J.G.; Lee, Y.B.; Jang, Y.P.; Oh, M.S. Protective effects of Belamcandae Rhizoma against skin damage by ameliorating ultraviolet-B-induced apoptosis and collagen degradation in keratinocytes. *Environ. Toxicol.* **2019**, *34*, 1354–1362. [CrossRef] [PubMed]
72. Chen, Y.M.; Liu, S.P.; Lin, H.L.; Chan, M.C.; Chen, Y.C.; Huang, Y.L.; Tsai, M.C.; Fu, R.H. Irisflorentin improves alpha-synuclein accumulation and attenuates 6-OHDA-induced dopaminergic neuron degeneration, implication for Parkinson's disease therapy. *Biomedicine* **2015**, *5*, 4. [CrossRef] [PubMed]
73. Fu, R.H.; Tsai, C.W.; Tsai, R.T.; Liu, S.P.; Chan, T.M.; Ho, Y.C.; Lin, H.L.; Chen, Y.M.; Hung, H.S.; Chiu, S.C.; et al. Irisflorentin modifies properties of mouse bone marrow-derived dendritic cells and reduces the allergic contact hypersensitivity responses. *Cell Transpl.* **2015**, *24*, 573–588. [CrossRef] [PubMed]
74. Gao, Y.; Fang, L.; Liu, F.; Zong, C.; Cai, R.; Chen, X.; Qi, Y. Suppressive effects of irisflorentin on LPS-induced inflammatory responses in RAW 264.7 macrophages. *Exp. Biol. Med.* **2014**, *239*, 1018–1024. [CrossRef]